Order Number 1346134

Some descriptors of the Markovian arrival process

Narayana, Surya, M.S.

The University of Arizona, 1991

U·M·I
300 N. Zeeb Rd.
Ann Arbor, MI 48106

SOME DESCRIPTORS OF THE MARKOVIAN ARRIVAL PROCESS

by

Surya Narayana

A Thesis Submitted to the Faculty of the

DEPARTMENT OF SYSTEMS AND INDUSTRIAL ENGINEERING

In Partial Fulfillment of the Requirements
For the Degree of

MASTER OF SCIENCE
WITH A MAJOR IN SYSTEMS ENGINEERING

In the Graduate College

THE UNIVERSITY OF ARIZONA

1991

STATEMENT BY AUTHOR

This thesis has been submitted in partial fulfillment of requirements for an advanced degree at The University of Arizona and is deposited in the University Library to be made available to borrowers under rules of the Library.

Brief quotations from this dissertation are allowable without special permission, provided that accurate acknowledgment of source is made. Requests for permission for extended quotation from or reproduction of this manuscript in whole or in part may be granted by the head of the major department or the Dean of the Graduate College when in his or her judgement the proposed use of the material is in the interests of scholarship. In all other instances, however, permission must be obtained from the author.

SIGNED: 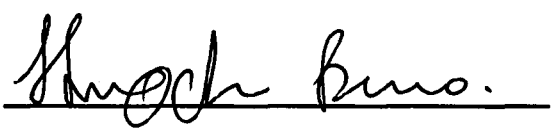

APPROVAL BY THESIS DIRECTOR

This thesis has been approved on the date shown below:

Marcel F. Neuts
Marcel F. Neuts
Professor of Systems and
Industrial Engineering

August 16, 1991
Date

Table of Contents

LIST OF ILLUSTRATIONS

ABSTRACT

The *Markovian Arrival Process* (*MAP*) is a tractable, versatile class of Markov renewal processes which has been extensively used to model arrival (or service) processes in queues. This thesis mainly deals with the first two moment matrices of the counts for the *MAP*. We derive asymptotic expansions for these two moment matrices and also derive efficient and stable algorithms to compute these matrices numerically. Simpler expressions for some of the classical mathematical descriptors of the superposition of independent *MAP*s also are derived.

CHAPTER 1

INTRODUCTION

This thesis deals with some descriptors of a useful class of random point processes. It is the initial stage of a larger study aimed at quantifying the effects of additional input streams on a single server queue. We first briefly review the basic properties of the *Markovian Arrival Process* (*MAP*). For this model, earlier studies of the classical mathematical descriptors of the process have been mostly restricted to the case when the stationary process is considered in a time interval starting at an arbitrary time or at an arbitrary arrival. These descriptors therefore record only the "average" behavior of the process. To remove this restriction on initial conditions means that we no longer have explicit analytic expressions for these descriptors; in particular there are no explicit expressions for two moment matrices: $M_1(t)$ and $M_2(t)$. We derive expressions for asymptotic expansions of these matrices and show how these can be used to study the asymptotic behavior of the process under different initial conditions. We derive efficient and stable algorithms to compute these two matrices numerically.

If the *MAP* being studied is the superposition of independent *MAP*s, then direct computation of descriptors of the process has two disadvantages: one, we may have to work with large matrices, and that we may lose sight of the properties of the component processes. By deriving simpler expressions for some descriptors of the superposition, we show how these disadvantages are overcome.

The *MAP* is a particularly tractable, versatile class of Markov renewal processes which has been extensively used as a model for arrival (or service) processes in queues. Detailed discussion may be found in Lucantoni [3], Lucantoni, Meier-Hellstern and Neuts [2], and Neuts [5], Neuts [6]. The *Markovian Arrival Process* is defined as the point process generated by the transition epochs of the m-state Markov renewal process with transition probability matrix

$$F(x) = \int_0^x \exp(D_0 u)du\ D_1, \quad \text{for } x \geq 0. \tag{1}$$

The square matrices D_0 and D_1 have the following properties:

a. $D_0 + D_1 = D$, an irreducible generator.

b. D_0 is a nonsingular matrix with negative diagonal elements and nonnegative off-diagonal elements.

c. D_1 is nonnegative.

The *PH* -renewal processes is a special *MAP*. To illustrate:

a. An Erlang renewal process of order three is represented by the parameter matrices

$$D_0 = \lambda_0 \begin{vmatrix} -1 & 1 & 0 \\ 0 & -1 & 1 \\ 0 & 0 & -1 \end{vmatrix}, \qquad D_1 = \lambda_0 \begin{vmatrix} 0 & 0 & 0 \\ 0 & 0 & 0 \\ 1 & 0 & 0 \end{vmatrix}.$$

b. A three stage hyperexponential renewal process is represented by

$$D_0 = \begin{vmatrix} -\lambda_1 & 0 & 0 \\ 0 & -\lambda_2 & 0 \\ 0 & 0 & -\lambda_3 \end{vmatrix}, \quad D_1 = \begin{vmatrix} \lambda_1\alpha_1 & \lambda_1\alpha_2 & \lambda_1\alpha_3 \\ \lambda_2\alpha_1 & \lambda_2\alpha_2 & \lambda_2\alpha_3 \\ \lambda_3\alpha_1 & \lambda_3\alpha_2 & \lambda_3\alpha_3 \end{vmatrix}.$$

A generalized form of the *MAP*, allowing for group arrivals is the *Batch Markovian Arrival Process* (*BMAP*). A detailed discussion of the *BMAP* can be found in [3]. The *BMAP* is defined by the parameter matrices D_k, $k \geq 0$ and the matrix

$$D = \sum_{k=0}^{\infty} D_k \tag{2}$$

is an irreducible infinitesimal generator. The matrix D_0 thus governs transitions that correspond to no arrival and D_j governs transitions that correspond to arrivals of batch size j. Let us denote by $N(t)$ the number of arrivals in the interval $(0,t)$. The (i,j)–th element of the matrix $P(n,t)$ is defined by

$$P_{i,(j)}(n,t) = P\{N(t) = n, J(t) = j \mid N(0) = 0, J(0) = i\}, \tag{3}$$

where $J(t)$ is the phase at time t. Then it is well known that the matrix generating function $P^*(z,t)$ defined by

$$P^*(z,t) = \sum_{n=0}^{\infty} P(n,t)z^n, \quad \text{for } |z| \le 1, \tag{4}$$

is explicitly given by

$$P^*(z,t) = \exp[D^*(z)t], \quad \text{for } |z| \le 1, \quad t \ge 0, \tag{5}$$

where the matrix generating function $D^*(z)$ is defined by

$$D^*(z) = \sum_{n=0}^{\infty} D_n z^n, \quad \text{for } |z| \le 1. \tag{6}$$

The matrices D_1^* and D_2^* are defined by

$$D_1^* = \sum_{n=1}^{\infty} nD_n = D^{*\prime}(1), \quad \text{and} \quad D_2^* = \sum_{n=1}^{\infty} n^2 D_n = D^{*\prime\prime}(1) + D^{*\prime}(1). \tag{7}$$

Next we shall review the basic properties of the *BMAP*. Classical mathematical descriptors of the *BMAP* may be computed using matrix-analytic formulas, which we shall review. In plotting the graphs of various descriptors, we shall use two specific examples. These are:

a. MAP(1) is an Erlang renewal process of order three defined by

$$D_0 = \begin{vmatrix} -3 & 3 & 0 \\ 0 & -3 & 3 \\ 0 & 0 & -3 \end{vmatrix}, \qquad D_1 = \begin{vmatrix} 0 & 0 & 0 \\ 0 & 0 & 0 \\ 3 & 0 & 0 \end{vmatrix}.$$

b. MAP(2) is defined by

$$D_0 = \lambda_0 \begin{vmatrix} -10 & 5 & 4 \\ 0 & -1 & 0 \\ 0 & 0 & -100 \end{vmatrix}, \qquad D_1 = \lambda_0 \begin{vmatrix} 1 & 0 & 0 \\ 0.5 & 0 & 0.5 \\ 10 & 0 & 90 \end{vmatrix}.$$

CHAPTER 2

BASIC PROPERTIES OF THE MARKOVIAN ARRIVAL PROCESS

The stationary probability vector of the irreducible generator D will be denoted by θ. The following are some well known properties of the *BMAP*.

a. The stationary version of the *BMAP* is obtained by choosing θ as the initial probability vector of the Markov renewal process. For the examples, θ is given by

$$\theta = [\ 0.333 \quad 0.333 \quad 0.333\ ] \quad \text{(Example } a.\text{)}$$

and

$$\theta = [\ 0.1504 \quad 0.7519 \quad 0.0977\ ] \quad \text{(Example } b.\text{)}$$

respectively.

b. The fundamental rate λ^* of the stationary point process is given by $\lambda^* = \theta D_1^* e$. Throughout e is a column vector of ones. Both examples will be normalized so that $\lambda^* = 1$. The *BMAP* of rate λ^* can be normalized to have rate one, merely by replacing D_k for all k *by* $\lambda^{*-1} D_k$. In Example *b*. this is achieved by setting $\lambda_0 = (10.67)^{-1}$.

c. We introduce the row vector **c** and the column vector **d** by

$$\mathbf{c} = \theta D_1^*(e\theta - D)^{-1}, \quad \text{and} \quad \mathbf{d} = (e\theta - D)^{-1}D_1^*e,$$

which recur in most of our formulas. The probability vector of the phase immediately following an arrival is given by

$$\theta_{arr} = \lambda^{*-1}[-\theta D_0]. \tag{8}$$

The Palm measure, $H(t) = E[N(t) \mid \text{arrival at } t = 0]$, the expected number of arrivals in an interval $(0,t)$ starting from an arbitrary arrival epoch, is given by the formula

$$H(t) = \lambda^* t + \theta_{arr}[I - \exp(Dt)]\mathbf{d}. \tag{9}$$

Upon differentiating in (9) we obtain the Palm density. Fig. 1 shows the graph of the Palm densities for Examples *a.* and *b.* We may rewrite (9) as

$$H(t) = \lambda^* t - \lambda^* + \theta_{arr}\mathbf{d} + \theta_{arr}[e\theta - \exp(Dt)]\mathbf{d}.$$

Since the last term tends to 0 as $t \to \infty$, the linear asymptote $h(t)$ of $H(\cdot)$ is given by

$$h(t) = \lambda^* t - \lambda^* + \theta_{arr}\mathbf{d}. \tag{10}$$

d. In the stationary version of the process the mean number of arrivals in an interval of length t is $\lambda^* t$ and the variance Var$[N(t)]$ of that count is given by

$$\text{Var}\,[N(t)] = [\lambda_2^* - 2\lambda^{*2} + 2\mathbf{c}D_1^*\mathbf{e}]t - 2\mathbf{c}[I - \exp(Dt)]\mathbf{d}, \tag{11}$$

where $\lambda_2^* = \boldsymbol{\theta}D_2^*\mathbf{e}$. By noting that $\mathbf{c}[\mathbf{e}\boldsymbol{\theta} - \exp(Dt)]\mathbf{d}$ tends to 0 as $t \to \infty$, we similarly obtain the linear asymptote $v(t)$ of Var$[N(t)]$:

$$v(t) = [\lambda_2^* - 2\lambda^{*2} + 2\mathbf{c}D_1^*\mathbf{e}]t + 2(\lambda^{*2} - \mathbf{cd}). \tag{12}$$

The dispersion function $I(t)$ is defined by $E[N(t)]^{-1}\text{Var}[N(t)]$. Graphs of Var$[N(t)]$ or $I(t)$ are widely used in applications to illustrate the variability of the number of events in a stationary process over an arbitrary time interval. Fig. 2 shows the graph of $I(t)$ for the examples.

e. The density $f(t)$ of the distribution of an arbitrary interarrival time is given by

$$f(t) = \boldsymbol{\theta}_{arr}\exp(D_0 t)(-D_0)\mathbf{e}. \tag{13}$$

Fig. 3 shows the graphs of $f(t)$ for the examples.

f. The covariance Cov(v;a) of the counts in the intervals $(0,a)$ and $(va, va + a)$ is given by

$$\mathrm{Cov}(v;a) = c[I - \exp(Da\,v)]d, \qquad v \geq 1. \tag{14}$$

$\mathrm{Var}[N(a)]^{-1}\mathrm{Cov}(v;a)$ is the correlation coefficient which will be denoted by $\rho_a(v)$. Figure 4 shows the graph of $\rho_a(v)$ for the examples.

g. The exponential peakedness function $z_{exp}(\mu)$ is the ratio of the variance and the mean of the number of busy servers in an infinite server queue to which the arrival process is hypothetically offered. A general discussion of peakedness may be found in Eckberg [1]. In terms of $\hat{H}(s)$, the Laplace-Stieltjes transform of the Palm measure $H(t)$, $z_{exp}(\mu)$ is given by

$$z_{exp}(\mu) = 1 + \hat{H}(\mu) - \mu^{-1}\lambda^*. \tag{15}$$

Fig. 5 shows the graphs of $z_{exp}(\mu)$ as a function of μ

In communications engineering the peakedness functional is used as a descriptor of second order properties of a point process. We note that this function if just another way of displaying the information contained in the Palm function $H(\cdot)$.

Although in both examples the fundamental rate is one, it is clear from Figs. 1-5 that there is marked difference between these two processes. In the Erlang renewal process, arrivals are fairly regularly spaced, whereas in *MAP*(2) there is wide variability in arrival rates; arrivals may occur in clusters, and the process is

more complex overall. These characteristics are brought out in the graphs. Clearly, each of these descriptors reveal *some* useful information about the process.

CHAPTER 3

THE MOMENTS OF THE COUNTING FUNCTION FOR THE BMAP

Let $X(t)$ denote the state of the *BMAP* at time t. We define the (i,j)-th element of the first and second factorial moment matrices $M_1(t)$ and $M_2(t)$ as follows:

$$[M_1(t)]_{i^*(j)} = E[N(t) \mid X(0) = i, X(t) = j]P\{X(t) = j \mid X(0) = i\}, \tag{16}$$

$$[M_2(t)]_{i^*(j)} = E[N(t)(N(t) - 1) \mid X(0) = i, X(t) = j]P\{X(t) = j \mid X(0) = i\}. \tag{17}$$

It is well known (see, for example, [5]) that $M_1(t)$ and $M_2(t)$ satisfy the differential equations

$$M_1'(t) = M_1(t)D + \exp(Dt)D_1^*, \qquad M_1(0) = 0, \tag{18}$$

$$M_2'(t) = M_2(t)D + 2M_1(t)D_1^* + \exp(Dt)(D_2^* - D_1^*), \qquad M_2(0) = 0. \tag{19}$$

Upon postmultiplying by $\exp(-Dt)$ in (18) and integrating, we obtain the formula

$$M_1(t) = \int_0^t \exp(Du)D_1^* \exp[D(t-u)]du. \tag{20}$$

Similarly upon postmultiplying by $\exp(-Dt)$ in (19) we get

$$M_2'(t)\exp(-Dt) - M_2(t)D\exp(-Dt) \tag{21}$$

$$= 2M_1(t)D_1^*\exp(-Dt) + \exp(Dt)(D_2^* - D_1^*)\exp(-Dt).$$

Upon integration it follows that

$$M_2(t) = 2\int_0^t M_1(u)D_1^*\exp[D(t-u)]du + \int_0^t \exp(Du)(D_2^* - D_1^*)\exp[D(t-u)]du$$

$$= 2\int_0^t\int_0^u \exp(Dv)D_1^*\exp[D(u-v)]dv\ D_1^*\exp[D(t-u)]du \tag{22}$$

$$+ \int_0^t \exp(Du)(D_2^* - D_1^*)\exp[D(t-u)]du.$$

Formulas (20) and (22) will be used to derive asymptotic expansions of the matrices $M_1(t)$ and $M_2(t)$ respectively. We will show that $M_1(t)$ has a linear asymptote in that there exist constant matrices A_0 and A_1 such that

$$M_1(t) = A_0 + A_1 t + O(e^{-\eta t}t^{2r+1}), \tag{23}$$

and that $M_2(t)$ has a quadratic asymptote in that there exist constant matrices B_0, B_1 and B_2 such that

$$M_2(t) = B_0 + B_1 t + B_2 t^2 + O(e^{-\eta t}t^{3r+2}), \tag{24}$$

where $-\eta$ is real part of η^*, the non-zero eigenvalue of D with maximum real part,

and

r is the multiplicity of η^*.

First we prove some preliminary results. The result in Lemma 1 is well-known. It is repeated here for completeness.

Lemma 1: As $t \to \infty$ we have the asymptotic formula

$$\exp(Dt) = \mathbf{e}\boldsymbol{\theta} + O(t^r e^{-\eta t}). \tag{25}$$

Proof: Writing $\exp(Dt)$ in its Jordan canonical form, we get

$$\exp(Dt) = H^{-1} \begin{vmatrix} 1 & 0 & 0 & . \\ 0 & e^{J_1 t} & 0 & . \\ 0 & 0 & e^{J_2 t} & . \\ . & . & . & . \end{vmatrix} H$$

where J_1 is the Jordan block for the eigenvalue η^* of multiplicity r. The matrix H has $\boldsymbol{\theta}$ as its first row and the matrix H^{-1} has $\mathbf{e}$ as its first column since $\boldsymbol{\theta}$ and $\mathbf{e}$ are the unique normalized left and right eigenvectors corresponding to the eigenvalue 0 of D. Therefore $\exp(Dt) = \mathbf{e}\boldsymbol{\theta} + H^{-1}\tilde{\Lambda}(t)H$, where

$$\tilde{\Lambda}(t) = \begin{vmatrix} 0 & 0 & 0 & . \\ 0 & e^{J_1 t} & 0 & . \\ 0 & 0 & e^{J_2 t} & . \\ . & . & . & . \end{vmatrix},$$

We observe that for any Jordan block J_j of order m_i corresponding to the eigenvalue η_i ,

$$e^{J_j t} = e^{\eta_i t} \sum_{k=0}^{m_i - 1} t^k A_{jk}, \tag{26}$$

where the A_{kj} are constant matrices.

If $\tilde{\Lambda}(t)$ has n Jordan blocks, then it follows from (26) that

$$H^{-1}\tilde{\Lambda}(t)H = \sum_{i=1}^{n} e^{\eta_i t} \sum_{k=0}^{m_i - 1} t^k B_{ik}, \tag{27}$$

where the B_{ik} are constant matrices. If η^* is the non-zero eigenvalue of D with largest real part having multiplicity r, then since the eigenvalues occur in complex conjugate pairs of the same multiplicity within each pair, it follows that

$$\left| \, e\theta - \exp(Dt) \, \right| < K_1 t^r e^{-\eta^* t}, \tag{28}$$

for some constant positive matrix K_1. •

The integration formula, see Neuts [7],

$$\int_0^t \exp(Du)du = e\theta t + [I - \exp(Dt)](e\theta - D)^{-1}, \tag{29}$$

will be frequently used in this section. A further integration formula is established in the next lemma.

Lemma 2:

$$\int_0^t v\exp(Dv)dv = \frac{1}{2}t^2 e\theta - t[\exp(Dt)(e\theta - D)^{-1} - e\theta] + [I - \exp[(Dt)](e\theta - D)^{-2}. \tag{30}$$

Proof:

$$\int_0^t v\exp(Dv)dv\ (e\theta - D) = \frac{1}{2}t^2 e\theta - \int_0^t v\exp(Dv)Ddv$$

$$= \frac{1}{2}t^2 e\theta - t\exp(Dt) + \int_0^t \exp(Dv)dv, \tag{31}$$

which upon substituting for the last integral from (29) and postmultiplying throughout by $(e\theta - D)^{-1}$ yields (30). •

Theorem 1: The matrix $M_1(t)$ has a linear asymptote $\tilde{M}_1(t)$ given by

$$\tilde{M}_1(t) = \lambda^* t e\theta + d\theta + ec - 2\lambda^* e\theta. \tag{32}$$

Proof: We rewrite (20) as

$$M_1(t) = \int_0^t \{e\theta - \exp(Du)\}D_1^*\{e\theta - \exp[D(t-u)]\}du - \lambda^* t e\theta \tag{33}$$

$$+ \int_0^t \exp(Du)du \; D_1^* e\theta + e\theta D_1^* \int_0^t \exp(Du)du.$$

Applying the triangle inequality to the first term and using Lemma 1, we obtain the following inequalities which hold element-wise:

$$\int_0^t \left| \{e\theta - \exp(Du)\} \right| D_1^* \left| \{e\theta - \exp[D(t-u)]\} \right| du$$

$$< \int_0^t K_1 D_1^* K_1 e^{-\eta u} u^r e^{-\eta(t-u)} (t-u)^r du \qquad (34)$$

$$= K_1 D_1^* K_1 e^{-\eta t} \int_0^t u^r (t-u)^r du \qquad < K_1 D_1^* K_1 e^{-\eta t} t^{2r+1}.$$

We make use of (29) to perform the necessary simplifications for the last two terms in (33) and we get

$$\left| M_1(t) - \lambda^* t e\theta - [I - \exp(Dt)]d\theta - ec[I - \exp(Dt)] \right| < K_1 D_1^* K_1 e^{-\eta t} t^{2r+1} \qquad (35)$$

Writing $[I - \exp(Dt]$ as $[I - e\theta] + [e\theta - \exp(Dt]$ and using Lemma 1 we get

$$\left| M_1(t) - \lambda^* t e\theta - ec - d\theta + 2\lambda^* e\theta \right|$$

$$< K_1 D_1^* K_1 e^{-\eta t} t^{2r+1} + ecK_1 e^{-\eta t} t^r + K_1 d\theta e^{-\eta t} t^r \qquad < K_2 e^{-\eta t} t^{2r+1}, \qquad (36)$$

where $K_2 = K_1 D_1^* K_1 + ecK_1 + K_1 d\theta$.

Therefore

$$M_1(t) = \lambda^* t e\theta + ec + d\theta - 2\lambda^* e\theta + O(e^{-\eta t} t^{2r+1}). \bullet \tag{37}$$

In the next two lemmas we establish further integration formulas needed in discussing the asymptotic expansion of $M_2(t)$.

Lemma 3:

$$\int_0^t M_1(u)du = \frac{1}{2}\lambda^* t^2 e\theta + t[d\theta + ec - 2\lambda^* e\theta] + \{3\lambda^* e\theta + (e\theta - D)^{-1}D_1^*(e\theta - D)^{-1} \tag{38}$$

$$- ec[I + (e\theta - D)^{-1}] - [I + (e\theta - D)^{-1}]d\theta\} + O(t^{2r+1}e^{-\eta t}).$$

Proof:

$$\int_0^t M_1(u)du = \int_0^t du \int_0^u \exp(Dv)D_1^* \exp[D(u-v)]dv \tag{39}$$

$$= \int_0^t \exp(Dv)D_1^*\, dv \int_0^{t-v} \exp(Du)du. \tag{40}$$

Upon integration carried out explicitly with the help of Lemma 3 and formula (29), we get

$$\int_0^t M_1(u)du = t\{e\theta t + [I - \exp(Dt)](e\theta - D)^{-1}\}D_1^* e\theta \tag{41}$$

$$- \{\frac{1}{2}t^2 e\theta + t[e\theta - \exp(Dt)](e\theta - D)^{-1} + [I - \exp(Dt)](e\theta - D)^{-2}\}D_1^* e\theta$$

$$+ \{e\theta t + [I - \exp(Dt)](e\theta - D)^{-1}\}D_1^*(e\theta - D)^{-1} - M_1(t)(e\theta - D)^{-1}$$

Upon substituting the terms on the right hand side by their asymptotic expansions, we get

$$\lambda^* t^2 e\theta + t[I - e\theta](e\theta - D)^{-1}D_1^* e\theta + O(e^{-\eta t}t^{r+1}) \tag{42}$$

$$- \frac{1}{2}\lambda^* t^2 e\theta - [I - e\theta](e\theta - D)^{-2}D_1^* e\theta + O(e^{-\eta t}t^{r+1})$$

$$+ ect + [I - e\theta](e\theta - D)^{-1}D_1^*(e\theta - D)^{-1} + O(e^{-\eta t}t^r)$$

$$- [\lambda^* te\theta + ec + d\theta - 2\lambda^* e\theta](e\theta - D)^{-1} + O(e^{-\eta t}t^{2r+1}).$$

Upon simplification and since $e^{-\eta t}t^{2r+1}$ is the dominant term among the O-terms, (38) follows. •

For convenience we define the vectors c_2 and d_2 by

$$c_2 = \theta(D_2^* - D_1^*)(e\theta - D)^{-1}, \quad \text{and} \quad d_2 = (e\theta - D)^{-1}(D_2^* - D_1^*)e. \tag{43}$$

Lemma 4:

$$\int_0^t \exp(Du)(D_2^* - D_1^*)\exp[D(t-u)]du \tag{44}$$

$$= \lambda_2 e\theta t + ec_2 + d_2\theta - 2\lambda_2 e\theta + O(e^{-\eta t}t^{2r+1}),$$

where $\lambda_2 = \theta(D_2^* - D_1^*)e$.

Proof: This is the same asymptotic expansion as used for $M_1(t)$ but with D_1^*

replaced by $D_2^* - D_1^*$. The stated formulas follow by routine calculations. •

Theorem 2 : $M_2(t)$ has a quadratic asymptote given by

$$\tilde{M}_2(t) = \lambda^{*2} t^2 e\theta + t\left[2\lambda^* d\theta + 2\lambda^* ec + e\theta[2cD_1^* e - 6\lambda^{*2} + \lambda_2]\right] \tag{45}$$

$$+\left[e\theta[12\lambda^{*2} - 2cd - 4cD_1^* e] - 4\lambda^* d\theta - 4\lambda^* ec + 2dc - 2\lambda^*[(e\theta - D)^{-1} d\theta + ec(e\theta - D)^{-1}]\right.$$

$$\left. + 2[ecD_1^*(e\theta - D)^{-1} + (e\theta - D)^{-1} D_1^* d\theta] + [ec_2 + d_2\theta - 2\lambda_2 e\theta]\right].$$

Proof: The second integral in (22) has been already evaluated in Lemma 4. The first term can be rewritten to get

$$2\int_0^t M_1(u) D_1^* \exp[D(t-u)]du = \tag{46}$$

$$2\int_0^t M_1(u) D_1^* e\theta du - 2\int_0^t M_1(u) D_1^* \{e\theta - \exp[D(t-u)]\} du.$$

The first integral can be obtained in a routine manner using Lemma 3. To obtain the second integral, we substitute $M_1(u)$ by its linear asymptote. The error in substituting the linear asymptote can be shown (using method similar to proof of Theorem 1) to be $O(t^{3r+2}e^{-\eta t})$. After performing the necessary simplifications, the dominant term among the O-terms is found to be $O(t^{3r+2}e^{-\eta t})$ and we obtain (45). •

In Chapter 5 we shall show how the asymptotic expansions of the factorial

moment matrices are useful in studying various descriptors of the *MAP* for different initial conditions.

CHAPTER 4

THE SUPERPOSITION

In this section we study the descriptors of the superposition of independent *MAP*s with single arrivals. If $[D_0(1), D_1(1)]$ of order m_1 and $[D_0(2), D_1(2)]$ of order m_2 are the parameter matrices of two independent *MAP*s with steady state vectors $\theta(1)$ and $\theta(2)$ respectively, it is well known that the superposition is also an *MAP* with the parameter matrices D_0 and D_1 and the invariant probability vector θ given by

$$D_0 = D_0(1) \oplus D_0(2) \quad \text{and} \quad D_1 = D_1(1) \oplus D_1(2), \tag{47}$$

$$\theta = \theta(1) \otimes \theta(2), \quad \text{and} \quad e = e(1) \otimes e(2).$$

The symbols $\otimes$ and $\oplus$ denote respectively the Kronecker product and sum of two matrices.

To evaluate descriptors of the superposition, such as the variance of $N(t)$, dispersion function, the Palm measure, the density of the interarrival time distribution, the renewal density and the peakedness, the formulas involve square matrices of order $m_1 m_2$ resulting in considerable computation time. Simpler expressions for these descriptors can, however, be obtained by careful conditioning of the various events in the process. We illustrate this method for a few descriptors. Graphs of these descriptors for the superposition of *MAP*(1) and *MAP*(2) are shown in Figures 6-10.

Let us denote the descriptor for the i–th process by superscript (i). We define the quantity p_i as the probability that an arbitrary arrival is from Stream i. Then if $\lambda^*_{(i)}$ is the fundamental rate for the i–th process, for a superposition of k *MAP*s obviously $p_i = \lambda^*_{(i)}(\sum_{j=1}^{k} \lambda^*_{(j)})^{-1}$.

By independence of the two processes, the variance $\mathrm{Var}[N(t)]$ and the dispersion function $I(t)$ for the superposition are clearly given by

$$\mathrm{Var}[N(t)] = \mathrm{Var}^{(1)}[N(t)] + \mathrm{Var}^{(2)}[N(t)], \tag{48}$$

$$I(t) = [(\lambda^*_{(1)} + \lambda^*_{(2)})t]^{-1}\{\mathrm{Var}^{(1)}[N(t)] + \mathrm{Var}^{(2)}[N(t)]\}. \tag{49}$$

Fig. 6 shows the graph of $I(t)$ for the superposition.

Theorem 3: For the superposition of two *MAP*s, the Palm measure $H(t)$ is given by

$$H(t) = p_1[H^{(1)}(t) + \lambda^*_{(2)}t] + p_2[H^{(2)}(t) + \lambda^*_{(1)}t]. \tag{50}$$

Proof: By conditioning on the arbitrary arrival at time $t = 0$ and using the law of total probability. •

Fig. 7 shows the plot of the superposition Palm density obtained by simply differentiating in (50). To derive a simpler expression for the density of the interarrival time distribution, we first define the conditional probabilities a_{11}, a_{12}, a_{21} and a_{22} as follows:

a_{11} = Prob. that starting with an arrival from Stream 1, there is no arrival from that stream in the interval $(0,t)$,

$$= \lambda_{(1)}^{*-1}\theta_1 D_1^{(1)} \exp[D_0^{(1)}t]e_1, \tag{51a}$$

a_{12} = Prob. that starting at an arbitrary instant, there is no arrival in the interval $(0,t)$ from Stream 2,

$$= \theta_2 \exp[D_0^{(2)}t]e_2, \tag{51b}$$

a_{21} = Prob. that starting at an arbitrary instant, there is no arrival in the interval $(0,t)$ from Stream 1,

$$= \theta_1 \exp[D_0^{(1)}t]e_1, \tag{51c}$$

a_{22} = Prob. that starting with an arrival from Stream 2, there is no arrival from that stream in the interval $(0,t)$,

$$= \lambda_{(2)}^{*-1}\theta_2 D_1^{(2)} \exp[D_0^{(2)}t]e_2. \tag{51d}$$

Theorem 4: The density $f(t)$ of the distribution of an arbitrary interarrival time is given by

$$f(t) = \{f^{(1)}(t)a_{12} + [\theta_2 \exp[D_0^{(2)}t]D_1^{(2)}e_2]a_{11}\}\, p_1 \tag{52}$$

$$+ \{f^{(2)}(t)a_{21} + [\theta_1 \exp[D_0^{(1)}t]D_1^{(1)}e_1]a_{22}\}\, p_2.$$

Proof: Let us first condition on the arrival at time $t = 0$. Let it be from Stream 1. Then $f^{(1)}(t)a_{12}dt$ and $[\theta_2 \exp[D_0^{(2)}t]D_1^{(2)}e_2]a_{11}dt$ are the respective elementary conditional probabilities that the next arrival occurs in the interval $(t, t + dt)$ from Stream 1 and Stream 2 respectively. Thus the first term within the parentheses in (52) is the conditional density of $f(t)$ given that the initial arrival is from Stream 1. We obtain an analogous expression by conditioning on the arrival at time $t = 0$ to be from Stream 2. Since p_1 and p_2 are the respective probabilities that the arrival at time 0 is from Stream 1 and Stream 2, we obtain the stated result by the law of total probability. •

The density $f(t)$ for the superposition is shown in Fig. 8.

Theorem 5: The exponential peakedness $z_{exp}(\mu)$ for the superposition of two *MAP*s is the weighted average of the exponential peakednesses of the individual processes, the weights being proportional to their fundamental rates, that is,

$$z_{exp}(\mu) = p_1 z_{1,exp}(\mu) + p_2 z_{2,exp}(\mu). \tag{53}$$

Proof: Taking the Laplace-Stieltjes transform of the Palm measure in (50) and replacing s by μ, we obtain

$$\hat{H}(\mu) = \left[\hat{H}_1(\mu) + \mu^{-1}\lambda_{(2)}^*\right]p_1 + \left[\hat{H}_2(\mu) + \mu^{-1}\lambda_{(1)}^*\right]p_2,$$

and substituting this value of $\hat{H}(\mu)$ in (6) we get

$$z_{exp}(\mu) = 1 + \left[\hat{H}_1(\mu) + \mu^{-1}\lambda_{(2)}^*\right]p_1 + \left[\hat{H}_2(\mu) + \mu^{-1}\lambda_{(1)}^*\right]p_2 - \mu^{-1}\lambda^*.$$

which when rewritten in terms of the individual exponential peakednesses gives the stated result. •

The superposition peakedness $z_{exp}(\mu)$ is shown in Fig. 9.

Let us consider two intervals of length a separated by a distance va ($v \geq 1$), having counts N_1 and N_2 respectively of the number of events in the stationary version of the *MAP*. The following theorem relates to the correlation $\rho_a(v)$ between N_1 and N_2.

Theorem 6: In the stationary version of the process, the correlation coefficient $\rho_a(v)$ for the superposition of two *MAP*s is the weighted mean of the individual correlation coefficients, the weights being proportional to their respective variances $\mathrm{Var}^{(i)}[N(t)]$, that is,

$$\rho_a(v) = \rho_a^{(1)}(v)\frac{\mathrm{Var}^{(1)}[N(t)]}{\mathrm{Var}[N(t)]} + \rho_a^{(2)}(v)\frac{\mathrm{Var}^{(2)}[N(t)]}{\mathrm{Var}[N(t)]}. \tag{54}$$

Proof: In the stationary version of the process, the variances $\mathrm{Var}[N_1(a)]$ and $\mathrm{Var}[N_2(a)]$ of the respective counts in the intervals $(0,a)$ and $(va, va + a)$ are equal. Therefore

$$\rho_a(v) = \frac{\mathrm{Cov}(v;a)}{\mathrm{Var}[N(a)]} = \frac{\mathrm{Cov}^{(1)}(v;a) + \mathrm{Cov}^{(2)}(v;a)}{\mathrm{Var}^{(1)}[N(a)] + \mathrm{Var}^{(2)}[N(a)]}.$$

since for the superposition, $\mathrm{Var}[N(a)]$ and $\mathrm{Cov}(v;a)$ are the respective sums. Rewriting the numerator in terms of the individual correlation coefficients,

$$\rho_a(v) = \frac{\rho_a^{(1)}(v)\mathrm{Var}^{(1)}[N(t)] + \rho_a^{(2)}(v)\mathrm{Var}^{(2)}[N(t)]}{\mathrm{Var}^{(1)}[N(a)] + \mathrm{Var}^{(2)}[N(a)]}. \tag{55}$$

The proof is complete since (54) and (55) are equivalent. •

The superposition correlation $\rho_a(v)$ is shown in Fig. 10.

The procedure described for the various descriptors is not limited to the superposition of just two *MAP*s, but can be easily extended to the superposition of k *MAP*s. The extension in the case of $\mathrm{Var}[N(t)]$, $\mathrm{Cov}(v;a)$, and $I(t)$ is trivial. For the others, the formulas are stated below.

$$H(t) = \lambda^* t + \sum_{i=1}^{k} p_i[H^{(i)}(t) - \lambda_{(i)}^* t]. \tag{56}$$

$$H'(t) = \lambda^* + \sum_{i=1}^{k} p_i[H'^{(i)}(t) - \lambda_{(i)}^*]. \tag{57}$$

$$z_{exp}(\mu) = \sum_{i=1}^{k} p_i z_{i,exp}(\mu). \tag{58}$$

$$\rho_a(v) = \sum_{i=1}^{k} \rho_a^{(i)}(v) \frac{\mathrm{Var}^{(i)}[N(a)]}{\sum_{i=1}^{k} \mathrm{Var}^{(i)}[N(a)]}. \tag{59}$$

For $k > 2$, the lengthy expression for $f(t)$ will be omitted. Although the results in this section have been stated for *MAP*s with single arrivals, they hold with minor modifications also for the *BMAP*s.

CHAPTER 5

PROCESS BEHAVIOR WITH DIFFERENT INITIAL CONDITIONS

Whereas in Chapter 2 and 4 we have examined stationary versions of the individual process and the superposition respectively, here we study the effect of other initial conditions on the descriptors of the *MAP*. In this respect one important use of the asymptotic expansions of $M_1(t)$ and $M_2(t)$ is brought out. Let $m_\alpha(t)$ be the linear asymptote of the expected number of arrivals in $(0,t)$, given that we start the process at time 0 according to the probability vector α. Then $m_\alpha(t)$ is given by

$$m_\alpha(t) = \lambda^* t + \alpha \mathbf{d} - \lambda^* \tag{60}$$

obtained by premultiplying by α and postmultiplying by $\mathbf{e}$ in (32) and simplifying. We see that (10) is the special case where $\alpha = \lambda^{*-1}(-D_0)\mathbf{e}$.

Similarly we have a general expression for the linear asymptote of the variance $v_\alpha(t)$ of $N(t)$, the number of arrivals in the interval $(0,t)$ for an arbitrary initial probability vector α. If we denote by $\mathrm{Var}_\alpha[N(t)]$ the variance of the count in the interval $(0,t)$ given that the process is started according to the initial vector α, then by definition

$$\mathrm{Var}_\alpha[N(t)] = \alpha M_2(t)\mathbf{e} + \alpha M_1(t)\mathbf{e} - [\alpha M_1(t)\mathbf{e}]^2. \tag{61}$$

Upon substituting for the asymptotes of $M_1(t)$ and $M_2(t)$ obtained in (32) and (45) and simplifying, we get

$$v_\alpha(t) = [2cD_1^*e - 2\lambda^{*2} + \lambda_2^*]t + B_0 + B_1(\alpha) \tag{62}$$

where

$$B_0 = 5\lambda^{*2} - 2cd - 2cD_1^*e - \lambda_2^*, \tag{63}$$

$$B_1(\alpha) = \alpha d - (\alpha d)^2 + 2\alpha(e\theta - D)^{-1}D_1^*d - 2\lambda^*\alpha(e\theta - D)^{-1}d + \alpha d_2.$$

An alternative way to obtain $v_\alpha(t)$ is to directly use row sum vectors of $M_1(t)$ and $M_2(t)$ which are already known (see proof of Theorem 7). We note in (62) that the linear term does not depend on the vector α.

We next study one important special case of Formula (62). By using the asymptotic expansions we establish the following result relating to the linear asymptote of $\mathrm{Var}[N_a(t)]$, the variance of the number of counts in the interval $(0,t)$ starting at an arbitrary arrival epoch.

Theorem 7: The linear asymptote $v_a(t)$ of $\mathrm{Var}[N_a(t)]$ is given by

$$v_a(t) = [2cD_1^*e - 2\lambda^{*2} + \lambda_2^*]t + \Big[5\lambda^{*2} - 2cd - 2cD_1^*e - \lambda_2^* \tag{64}$$

$$+ \theta_{arr}[d + 2(e\theta - D)^{-1}D_1^*d - 2\lambda^*(e\theta - D)^{-1}d - \theta_{arr}dd + d_2]\Big].$$

Proof: Since θ_{arr} specifies the phase of the *MAP* at an arbitrary arrival,

$$\mathrm{Var}[N_a(t)] = \theta_{arr}M_2(t)e + \theta_{arr}M_1(t)e - [\theta_{arr}M_1(t)e]^2. \tag{65}$$

As shown in [7] the row sum vectors $M_1(t)\mathbf{e}$ and $M_2(t)\mathbf{e}$ are given by the formulas

$$M_1(t)\mathbf{e} = \lambda^* t\mathbf{e} + [I - \exp(Dt)](\mathbf{e}\theta - D)^{-1}D_1^*\mathbf{e}, \tag{66a}$$

$$M_2(t)\mathbf{e} = \lambda^{*2}t^2\mathbf{e} + 2t\theta D_1^*(\mathbf{e}\theta - D)^{-1}D_1^*\mathbf{e}\,\mathbf{e} \tag{66b}$$

$$- 2(\mathbf{e}\theta - D)^{-1}\{M_1(t) - D_1^*\int_0^t \exp(Du)du\}D_1^*\mathbf{e} - 2\theta D_1^*\int_0^t \exp(Du)du\,(\mathbf{e}\theta - D)^{-1}D_1^*\mathbf{e}\,\mathbf{e}.$$

Upon substituting the asymptotic value of $M_1(t)$ obtained in (32) into (66b) and simplifying the remaining terms in (65) the result follows. •

Fig. 11 and Fig. 12 shows the graph of $\mathrm{Var}[N_a(t)]$ for the Examples *a.* and *b.*

Next we look at the behavior of the process over an arbitrary time interval with different initial conditions. This means that instead of starting the process according to the steady state vector θ or according to θ_{arr}, we start the process according to an arbitrary probability vector α. With this initial condition we evaluate various descriptors such as those discussed in Chapter 2. To do that we want computable expressions with the given initial conditions for the various descriptors. In most cases there are no explicit analytic expressions but the quantities are computed by numerical methods.

To illustrate, $\mathrm{Var}_\alpha[N(t)]$, the variance of the counts in the interval $(0,t)$ given that the process is started according to the vector α is given by

$$\mathrm{Var}_{\alpha}[N(t)] = \alpha M_2(t)\mathbf{e} + \alpha M_1(t)\mathbf{e} - [\alpha M_1(t)\mathbf{e}]^2. \tag{67}$$

Similarly, the covariance $\mathrm{Cov}_{\alpha}(v;a)$, the correlation coefficient $\rho_{a,\alpha}(v)$ and the density $f_{\alpha}(t)$ of the distribution of interarrival time are given by

$$\mathrm{Cov}_{\alpha}(v;a) = \alpha M_1(a)\exp(Dt)M_1(a)\mathbf{e} \tag{68}$$

$$- \Big[\alpha M_1(a)\mathbf{e}\Big]\Big[\alpha\exp[D(t+a)]M_1(a)\mathbf{e}\Big],$$

$$\rho_{a,\alpha}(v) = \mathrm{Cov}_{\alpha}(v;a)\Big[\alpha M_2(a)\mathbf{e} + \alpha M_1(a)\mathbf{e} - [\alpha M_1(a)\mathbf{e}]^2\Big]^{-\frac{1}{2}} \tag{69}$$

$$\cdot\Big[\alpha\exp[D(t+a)]M_2(a)\mathbf{e} + \alpha\exp[D(t+a)]M_1(a)\mathbf{e}$$

$$- [\alpha\exp(D(t+a))M_1(a)\mathbf{e}]^2\Big]^{-\frac{1}{2}}.$$

$$f_{\alpha}(t) = \alpha\exp(D_0 t)(-D_0)\mathbf{e}. \tag{70}$$

In (70) we see that α_j, the j–th element of α is zero if there are no transitions into state j upon an arrival. Therefore (70) is defined only if

$$\alpha_j = 0 \quad \text{when the } j\text{–th element of } \mathbf{e}^T(D_1 - D_0) = 0. \tag{71}$$

We can proceed in a similar manner for the other descriptors described in Chapter 2; and may easily extend these formulas for the superposition.

In evaluating the above quantities, the matrix exponential, and the first and second factorial moment matrices are to be numerically computed. Algorithms for the computation

of the matrix exponential and the algorithms for computing $M_1(t)$ and $M_2(t)$ for the *MAP* are described in the next section.

CHAPTER 6

COMPUTATION OF FIRST AND SECOND FACTORIAL MOMENT MATRICES

Computation of the matrix exponential: We discuss briefly the *uniformization* method. The matrix $\exp(Dt)$ can be rewritten as

$$\exp(Dt) = [\exp(D\tau)]^k \qquad \text{where } \tau = k^{-1}t, \quad \text{for all } k \geq 1. \tag{72}$$

The method therefore essentially involves computing $\exp(D\tau)$ to high accuracy for a sufficiently small value of τ. To avoid loss of significance, we write

$$\exp(D\tau) = e^{-c\tau}\sum_{n=0}^{\infty}\frac{(c\tau)^n}{n!}K^n \tag{73}$$

where K is the stochastic matrix $c^{-1}D + I$ and c is the absolute value of the smallest diagonal element in D. It is well known (see, for example [4]) that

$$K^n = e\theta + O(\eta^n) \tag{74}$$

where $\eta < 1$ is the modulus of the second largest eigenvalue of K.

Therefore if we truncate the series in (73) at a suitably high value N, the error in truncation given by

$$E_0 = e^{-c\tau}\sum_{n=N+1}^{\infty}\frac{(c\tau)^n}{n!}K^n \tag{75}$$

behaves like that of the Poisson density. By choosing τ sufficiently small, we can compute $\exp(D\tau)$ to high accuracy with a modest number of terms. Then we may obtain $\exp(Dt)$ for higher values of t using formula (72).

The first and second factorial moment matrices $M_1(t)$ and $M_2(t)$ can be efficiently computed by truncating the infinite series involved and making use of recurrence relations at various stages in the computations. The essential steps are shown below.

Theorem 8: For the *MAP* with group arrivals , $M_1(t)$ is given by

$$M_1(t) = e^{-ct} \sum_{n=0}^{\infty} \frac{(ct)^{n+1}}{(n+1)!} E(n) \tag{76}$$

where $E(k+1) = KE(k) + c^{-1}D_1^* K^{k+1}, \quad E(0) = c^{-1}D_1^*.$ (77)

Proof: To evaluate the integral in (20), the matrix exponentials in the integrand are substituted by their respective expansions as in (73) and we get that

$$M_1(t) = e^{-ct} \int_0^t \sum_{n=0}^{\infty} \frac{(cu)^n}{n!} K^n D_1^* \sum_{m=0}^{\infty} \frac{(c(t-u))^m}{m!} K^m du \tag{78}$$

$$= c^{-1}e^{-ct} \sum_{n=0}^{\infty} \sum_{m=0}^{\infty} \frac{(ct)^{m+n+1}}{(m+n+1)!} K^n D_1^* K^m \quad = c^{-1}e^{-ct} \sum_{n=0}^{\infty} \sum_{m=0}^{n} \frac{(ct)^{n+1}}{(n+1)!} K^m D_1^* K^{n-m}.$$

Writing $E(k)$ for the term $\sum_{m=0}^{k} K^m c^{-1} D_1^* K^{k-m}$, we have the recurrence relation $E(k+1) = KE(k) + c^{-1}D_1^* K^{k+1}, \quad E(0) = c^{-1}D_1^*$, and therefore

$$M_1(t) = e^{-ct} \sum_{n=0}^{\infty} \frac{(ct)^{n+1}}{(n+1)!} E(n). \bullet \tag{79}$$

Theorem 9: For the *MAP* with group arrivals, $M_2(t)$ is given by

$$M_2(t) = 2e^{-ct} \sum_{n=0}^{\infty} \frac{(ct)^{n+2}}{(n+2)!} G(n) + e^{-ct} \sum_{n=0}^{\infty} \frac{(ct)^{n+1}}{(n+1)!} L(n). \tag{80}$$

where $G(k+1) = c^{-1}D_1^* E(k+1) + KG(k), \quad G(0) = c^{-2}D_1^{*2}, \tag{81}$

and $L(k+1) = c^{-1}(D_2^* - D_1^*)L(k) + c^{-1}(D_2^* - D_1^*)K^{k+1}, \quad L(0) = c^{-1}(D_2^* - D_1^*).$

Proof: For the *MAP* with group arrivals we have from (22) that

$$M_2(t) = 2\int_0^t \int_0^u \exp(Dv) D_1^* \exp(D(u-v)) D_1^* \exp(D(t-u)) dv\ du$$

$$+ \int_0^t \exp(Du)(D_2^* - D_1^*) \exp[D(t-u)] du.$$

The similarity of the second term in the above expression with the expression on the right hand side in (20) is obvious. The corresponding steps in the calculations follow routinely from the proof of Theorem 8 upon replacing D_1^* by $(D_2^* - D_1^*)$. The first term, using the same expansion (73) for the matrix exponentials

$$= 2\, e^{-ct} \sum_{k=0}^{\infty} \sum_{v=0}^{\infty} \sum_{r=0}^{\infty} \int_0^t \int_0^u \frac{(cv)^k}{k!} \frac{(c(u-v))^v}{v!} \frac{(c(t-u))^r}{r!} dv\ du\ K^k D_1^* K^v D_1^* K^r$$

$$= 2e^{-ct} c^{-2} \frac{(ct)^{k+v+r+2}}{k!v!r!} \int_0^1 \int_0^u v^k (u-v)^v (1-u)^r du\ dv\ K^k D_1^* K^v D_1^* K^r$$

$$= 2c^{-2}\sum_{k=0}^{\infty}\sum_{v=0}^{\infty}\sum_{r=0}^{\infty} e^{-ct}\frac{(ct)^{k+v+r+2}}{(k+v+r+2)!}K^k D_1^* K^v D_1^* K^r$$

$$= 2c^{-2}\sum_{n=0}^{\infty} e^{-ct}\frac{(ct)^{n+2}}{(n+2)!}\sum_{k=0}^{n}\sum_{r=0}^{k} K^r D_1^* K^{k-r} D_1^* K^{n-k}. \tag{82}$$

Setting $G(k) = \sum_{k=0}^{n}\sum_{r=0}^{k} K^r c^{-1} D_1^* K^{k-r} c^{-1} D_1^* K^{n-k}$, we have the recurrence relation

$$G(k+1) = c^{-1}D_1^* E(k+1) + KG(k), \quad G(0) = c^{-2}D_1^{*2},$$

and (82) becomes

$$2\sum_{n=0}^{\infty} e^{-ct}\frac{(ct)^{n+2}}{(n+2)!}G(n).$$

Therefore

$$M_2(t) = 2e^{-ct}\sum_{n=0}^{\infty}\frac{(ct)^{n+2}}{(n+2)!}G(n) + e^{-ct}\sum_{n=0}^{\infty}\frac{(ct)^{n+1}}{(n+1)!}L(n). \bullet$$

The matrices $E(n)$, $G(n)$ and $L(n)$ can be computed in a routine manner by using the recurrence relations given in (76) and (80). Therefore, upon suitably truncating the series in (77) and (81), we can compute $M_1(t)$ and $M_2(t)$. The next theorem is used to analyze the errors

$$E_1 = \sum_{k=N+1}^{\infty} e^{-ct}\frac{(ct)^{k+1}}{(k+1)!}E(k), \tag{83}$$

$$E_2 = 2\sum_{k=N+1}^{\infty} e^{-ct}\frac{(ct)^{k+2}}{(k+2)!}G(k) + \sum_{k=N+1}^{\infty} e^{-ct}(ct\frac{)^{k+1}}{(k+1)!}L(k) \tag{84}$$

in truncating the series in (76) and (80).

Theorem 10: The error terms E_1 and E_2 are given by

$$E_1 = \sum_{k=N+1}^{\infty} e^{-ct}\frac{(ct)^{k+1}}{(k+1)!}[k\lambda^* c^{-1}e\theta + o(k)], \tag{85a}$$

$$E_2 = 2\sum_{k=N+1}^{\infty} e^{-ct}\frac{(ct)^{k+2}}{(k+2)!}[k^2\lambda^{*2}c^{-2}e\theta + o(k^2)] \tag{85b}$$

$$+ \sum_{k=N+1}^{\infty} e^{-ct}\frac{(ct)^{k+1}}{(k+1)!}[k\lambda_2 c^{-1}e\theta + o(k)],$$

Proof: For convenience let us denote the first and second terms in (86) by E_{21} and E_{22} respectively. We will prove that

$$E_{21} = 2\sum_{k=N+1}^{\infty} e^{-ct}\frac{(ct)^{k+2}}{(k+2)!}[k^2\lambda^{*2}c^{-2}e\theta + o(k^2)] \tag{86}$$

The remaining part of the proof is apparent once (86) is proved. To prove (86), we have

$$n^{-2}G(n) = n^{-2}\sum_{k=0}^{n}\sum_{r=0}^{k} K^r c^{-1}D_1 K^{k-r}c^{-1}D_1 K^{n-k} \tag{87}$$

$$= n^{-2}\sum_{k=0}^{j}\sum_{r=0}^{k} K^r c^{-1}D_1 K^{k-r}c^{-1}D_1 K^{n-k} + n^{-2}\sum_{k=j+1}^{n}\sum_{r=0}^{k} K^r c^{-1}D_1 K^{k-r}c^{-1}D_1 K^{n-k}, \tag{88}$$

which on rewriting

$$= n^{-2} \sum_{k=0}^{j} \sum_{r=0}^{k} K^r c^{-1} D_1 K^{k-r} c^{-1} D_1 K^{n-k} \tag{89}$$

$$+ n^{-2} \tilde{K} G(n-j-1)] + n^{-2}(K^{j+1} - \tilde{K}) G(n-j-1),$$

where $\tilde{K}$ is the matrix $\mathbf{e}\theta$.

We first show that $\{k^{-2}G(k)\}$ is bounded. To see this, we form the product

$$\theta[k^{-2}G(k)]\mathbf{e} = k^{-2}\theta D_1^* \sum_{v=0}^{k} \sum_{r=0}^{v} K^{v-r} D_1^* \mathbf{e},$$

which is bounded, since

$$k^{-2} \sum_{v=0}^{k} \sum_{r=0}^{v} K^r \mathbf{e} = \frac{k-1}{2k} \mathbf{e}.$$

By choosing j sufficiently large, the third term in the second form in (XX) therefore can be made arbitrarily small. For any fixed j, the first term is arbitrarily small for k sufficiently large. Since the sequence of positive matrices $\{k^{-1}E(k)\}$ is bounded (by the same argument as given earlier,) the last term can be made arbitrarily small for every fixed j by choosing k sufficiently large.

Finally, it is readily seen that the second term $k^{-2}\mathbf{e}\theta G(k-j-1)$ converges to

$$c^{-2}\mathbf{e}\theta D_1^* \mathbf{e}\theta D_1^* \mathbf{e}\theta = c^{-2}\lambda^{*\,2}\mathbf{e}\theta, \tag{91}$$

On substituting for $G(k)$ in the expression for E_{21}, we obtain (86). •

If we define A_1 to be slightly larger than $2\lambda^{*2}c^{-2}e\theta$, then

$$E_{21} < A_1(ct)^2 e^{-ct} \sum_{k=N+1}^{\infty} \frac{(ct)^k}{k!} \tag{XX}$$

and so we see that the error term E_{21} behaves like that for the Poisson density. A similar result holds for E_{22} and E_1.

The following addition formulas enable recursive computation of $M_1(n\tau)$ and $M_2(n\tau)$ for various values of n, starting from $M_1(\tau)$, $M_2(\tau)$.

$$M_1(t_1 + t_2) = M_1(t_1)\exp(Dt_2) + \exp(Dt_1)M_1(t_2), \tag{93}$$

$$M_2(t_1 + t_2) = M_2(t_1)\exp(Dt_2) + 2M_1(t_1)M_1(t_2) + \exp(Dt_1)M_2(t_2).$$

From these it readily follows that

$$M_1(n\tau) = M_1[(n-1)\tau]\exp(D\tau) + \exp[D(n-1)\tau]M_1(\tau), \tag{94}$$

$$M_2(n\tau) = M_2[(n-1)\tau]\exp(D\tau) + 2M_1[(n-1)\tau]M_1(\tau) + \exp[D\tau(n-1)]M_2(\tau). \tag{95}$$

Procedure for numerical computation: From Theorem 10 it is clear that the series in (76) and (80) behave in a stable manner, and since the error terms behave like those for the Poisson density, we can compute $M_1(\tau)$ and $M_2(\tau)$ from (76) and (80) respectively by truncating the series involved at a suitable value N such that the difference in the respective row sums is of very small magnitude. The number of terms required to achieve a

desired accuracy for a fixed τ will depend upon the sequence of matrices D_k but we can always select a suitably small interval τ over which we can compute to high accuracy with a modest number of terms. Then we use the recursive relations (94) and (95) to compute over increasingly larger intervals.

CHAPTER 7

NUMERICAL EXAMPLES

To illustrate the effect of initial conditions on the superposition, the following *MAP*s are used as examples.

Example (*i*) is a superposition of two identical *MAP*s with the matrices D_0 and D_1 given by

$$\begin{aligned} D_0(i,i) &= -2, \quad \text{for } 1 \le i \le 20, \\ D_0(i,i+1) &= 1.8, \quad \text{for } 1 \le i \le 10, \\ &= 0.2, \quad \text{for } 11 \le i \le 19, \\ D_0(20,1) &= 0.2, \end{aligned}$$

$$\begin{aligned} D_1(i,i+1) &= 0.2 \quad \text{for } 1 \le i \le 10, \\ &= 1.8, \quad \text{for } 11 \le i \le 19, \\ D_1(20,1) &= 1.8. \end{aligned}$$

All other elements of D_0 and D_1 are zero.

Example (*ii*) is a superposition of two identical *MAP*s with D_0 and D_1 given by

$$\begin{aligned} D_0(i,i) &= -10\lambda_0, \quad \text{for } 1 \le i \le 15, \\ D_0(i,i+1) &= 9\lambda_0, \quad \text{for } 6 \le i \le 10, \\ &= 10\lambda_0, \quad \text{for } 11 \le i \le 15, \\ D_0(15,1) &= D_0(15,6) = 5\lambda_0. \end{aligned}$$

$$D_1(i,i+1) = 10\lambda_0, \quad \text{for } 1 \le i \le 5,$$

$$= \lambda_0, \quad \text{for } 6 \le i \le 10.$$

with $\lambda_0 = (2.4)^{-1}$. All other elements are zero.

Example (*iii*) has the coefficient matrices

$$D_0^{(1)}(i,i) = -10\lambda_0, \quad \text{for } 1 \le i \le 15,$$
$$D_0^{(1)}(i,i+1) = 0.5\lambda_0, \quad \text{for } 1 \le i \le 2,$$
$$= 10\lambda_0, \quad \text{for } 3 \le i \le 15,$$

$$D_1^{(1)}(i,i+1) = 9.5\lambda_0, \quad \text{for } 1 \le i \le 2,$$

with $\lambda_0 = (1.267)^{-1}$ and

$$D_0^{(1)} = \begin{vmatrix} -10\lambda_0 & 10\lambda_0 \\ 0 & -100\lambda_0 \end{vmatrix}, \qquad D_1^{(2)} = \begin{vmatrix} 0 & 0 \\ 0.5\lambda_0 & 99.5\lambda_0 \end{vmatrix}.$$

with $\lambda_0 = (95.24)^{-1}$. Each of these *MAP*s are time scaled so that the fundamental rate λ^* is one. In all examples the initial probability vector α is of the form

$$\alpha = [\, 0, \ldots 0, 1, 0, \ldots 0 \,],$$

so that a specific initial state is chosen. Three descriptors, $\rho_\alpha(v)$, $I_\alpha(t)$ and $H'_\alpha(t)$ will be examined for each of the examples. Figs. 13-21 show these descriptors for different choices of the vector α. For convenience the graph where the first process is started in Phase i and the second process in Phase j will be labeled (i,j).

Discussion of the examples: The three examples have intentionally been chosen so that the physical behavior of the various *MAP*s can easily be visualized. By choosing various initial conditions and by examining the computed descriptors, we can gain an understanding of the behavior of the superposition when we focus on portions of the path functions which start with these selected initial conditions.

Example (*i*) can be constructed starting with a Poisson process of rate 2. Blocks of ten successive points are considered and some points within each block are deleted. We perform 10 Bernoulli trials for each block and in these, alternatingly use a probability 1/10 or 9/10 to preserve a point. The process of the preserved points is the *MAP* with the given parameter matrices. A typical realization of the point process will show alternating time intervals with many and few points.

When both component processes are started in the Phase 1, the graph of $H'_{\alpha}(t)$ (solid line) shown in Figure 13 initially shows peaks and valleys corresponding to the times periods when both processes have many or few points. Similarly, when both processes start in the Phase 10, the high initial peak of the graph represents the coinciding "bursts" in the two processes. The peaks and valleys of that curve appear substantially at the same times, but inversely to the case where both component processes start out with a "sparse" interval. The Palm density, which corresponds to time $t = 0$ chosen at an arbitrary arrival is much less variable.

It show peaks and valleys which appear roughly midway between those in the preceding two cases. When one process starts in Phase 1 and the other in Phase 11 the corresponding $H'_a(t)$ (dotted line) is almost constant at 2. The asymptotic behavior of all four curves is similar and suggests that the effect of the initial conditions is fully attenuated after some 40 time units.

The graphs of the dispersion curves (Figure 14) show the same behavior, but since the dispersion curves are "smoother" they show less detail. In general, we find graphs of $H'_a(t)$ to be more easily interpretable than those of corresponding dispersion functions.

Since the correlation coefficient depends on Cov(v;a), Var[$N_1(a)$] and Var[$N_2(a)$], graphs of $\rho_a(v)$ (Figures 15, 18 and 21) are, in general, not so easily interpretable. The value of "a" in this case is 1.0 which is twice the mean sojourn time in one state of the component process. In Figure 15 the graph of (10,10) drops sharply to a negative correlation of about 0.2 and this corresponds to the low number of counts in Phases 1 to 10 following the high arrival rate in Phases 11 to 20. The graph of (1,11) shows a sort of intermediate behavior when compared to the graphs of (1,1) and (10,10), just as in the graphs of $H'_a(t)$.

Example (*ii*) can be constructed as follows. We start with a Poisson process of rate $10\lambda_0$. We consider blocks of 5 successive points each. We preserve all

5 points in the first block. Then we perform Bernoulli trials for each of the next 5 points with probability 1/10 of preserving a point. All 5 points in the third block are deleted. Finally, with equal probability we move either to the first block or second block. The process of the preserved points is one of the component *MAP*s with the given parameter matrices.

All graphs in Figures 16-18 show that the effect of initial conditions lasts for about 13 time units only. Thus, the effect on the descriptor of a "bursty" or a "sparse" interval is for a short time only, corresponding to a lesser degree of memory in the process, as compared with the previous example. The initial valley followed by the peak in the graph of (5,5) of $H'_{\alpha}(t)$ (Figure 16) corresponds to the low arrival rate in Phases 5 to 15 followed by a "burst". A lesser variability is seen in the graph of (5,15) and the graph corresponding to the Palm density is even smoother.

The value of the dispersion function in any interval depends on the expected number of counts and the corresponding variance of counts in that interval. When both processes are started in Phase 5, the initial drop in the graph of the dispersion function in Figure 17 corresponds to the interval when both processes are in Phases 5 to 10 and the process is more "regular". Subsequently, the variability increases while the expected number of counts does not proportionately increase and this is reflected by the sharp rise in the same graph. After about 4 time units,

the effect of initial conditions becomes very small; the graphs become much smoother and converge to the constant asymptotic value of 1.59.

In Figure 18, the large initial negative correlation shown in the graph of (5,5) corresponds to a higher probability of arrivals initially, in contrast to that in the subsequent intervals of length $a = 0.25$. Upon leaving Phase 15, with equal probability, there is either a "burst" of arrivals (corresponding to Phases 1 to 5) or a "sparse" interval (corresponding to Phases 6 to 10). This is reflected in the initial positive correlation in the graph corresponding to (15,15). An intermediate sort of behavior between the preceding cases (dashed line) is seen when one process is started in Phase 5 and the other in Phase 15.

Example (*iii*) is a superposition of two *MAP*s, where *MAP*(1) describes a process moving in a cyclic manner with the same mean sojourn time through 15 states; when there is a transition from Phases 1 or 2 a point is generated with probability 19/20. *MAP*(2) is an interrupted Poisson process where the mean sojourn times in Phases 1 and 2 are approximately 9 and 190 respectively, and in Phase 2 arrivals are generated according to a Poisson process of rate approximately 1.

Therefore, a typical realization of *MAP*(1) consists of "bursts" of one or two points in quick succession separated from the next such "burst" by a fairly large gap. In the second process, we typically see long intervals in which points

are generated according to a Poisson process, followed by shorter intervals without arrivals. When the two processes are started in Phases 2 and 1 respectively, the corresponding $H'_{\alpha}(t)$ (Figure 19) is initially unaffected by *MAP*(1) (solid line). After about 3 time units the effect of arrivals in *MAP*(2) is seen in the upward trend of the same graph. When *MAP*(2) is started in Phase 2, the resultant process is just *MAP*(1) upon which is superimposed a Poisson process. This explains why the peaks and valleys corresponding to "bursts" and "sparse" intervals appear at the same time in the graph of (2,1) as in (3,2) but the graph is "shifted" upward. Since the steady state vector at arrivals of *MAP*(2) has the value [0.005 0.995], the graph corresponding to the Palm density is roughly similar to the graph of (3,2).

The effect of the uniform arrival rate in Phase 2 of *MAP*(2) is shown by the dispersion function graph (dashed line) of (3,2) in Figure 20. In contrast the sharp peak in the graph of (2,1) corresponds to a "sparse" interval. The smooth behavior thereafter corresponds to the sojourn in Phase 2 of *MAP*(2). We observe also that in the graphs of (3,2) and the stationary version the asymptotic behavior can be clearly seen, while the graph of (2,1) converges much more slowly to the asymptotic value of 0.99. The effect of *MAP*(1) is not visible in the graphs because of the large time scale chosen.

When *MAP*(1) and *MAP*(2) are started in Phases 3 and 2 respectively, the corresponding graph (dotted line) in Figure 21 shows zero correlation coefficient.

This is not astonishing and is explained as follows. In the initial interval corresponding to the sojourn in Phases 3 to 15 of *MAP*(1) there are no arrivals and the superposition therefore initially behaves almost like a Poisson process because of the long sojourn time in Phase 2 of *MAP*(2). Since *MAP*(2) is in Phase 2 most of the time, this effect is seen in all the graphs, which converge quickly to zero after an initial fluctuation. The large negative correlation seen in the graph of (2,1) corresponds to the high probability of an arrival in Phase 2 of *MAP*(2).

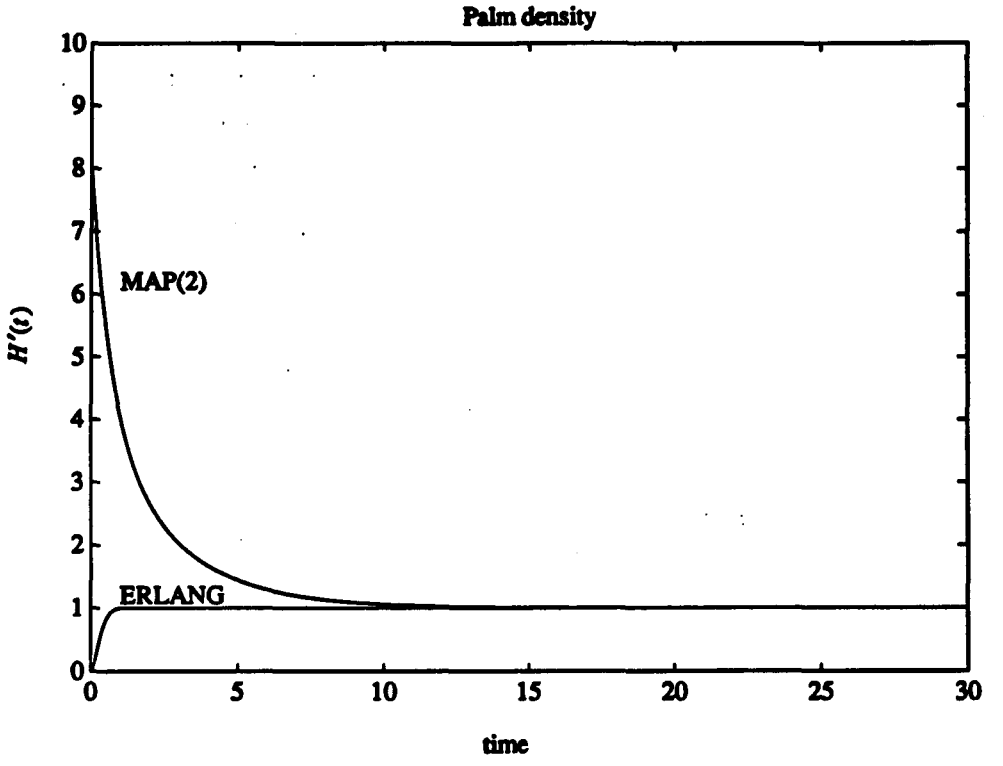

Figure 1: Palm density for Examples a. and b.

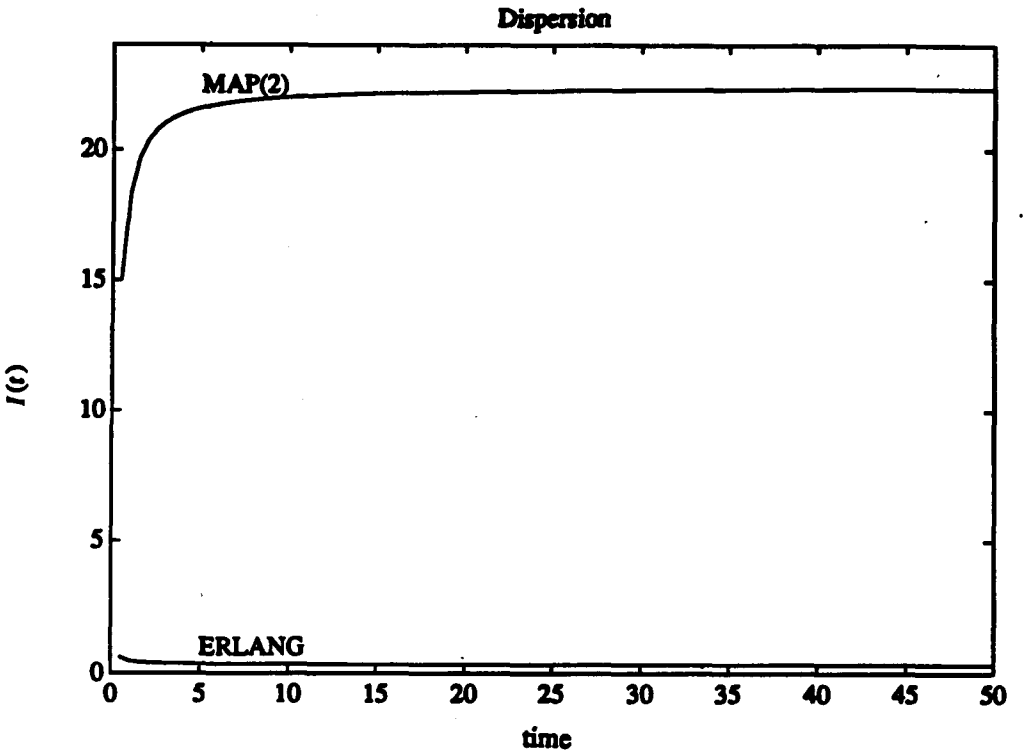

Figure 2: Dispersion function for Examples a. and b.

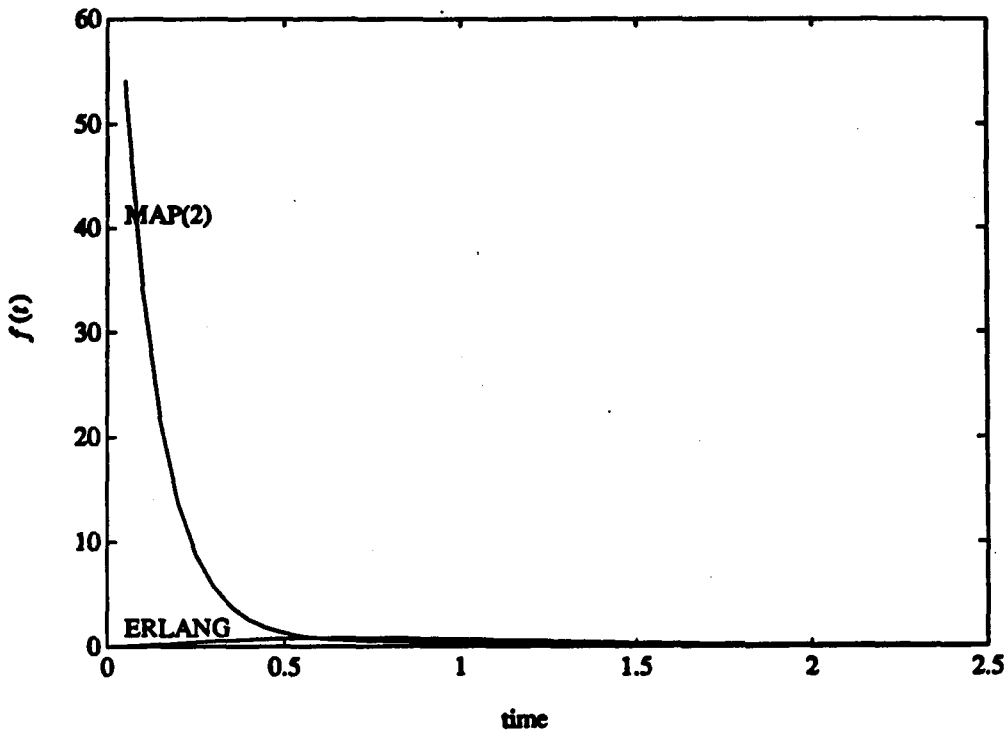

Figure 3: Density of the distribution of an arbitrary interarrival time

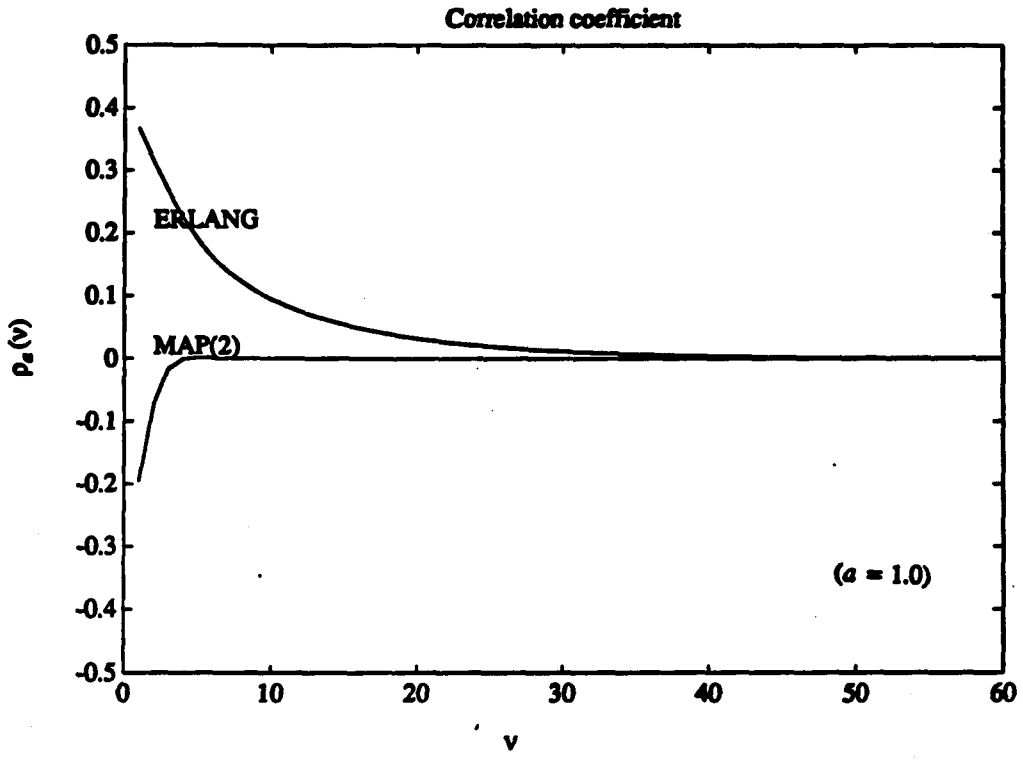

Figure 4: Correlation coefficient for Examples a. and b.

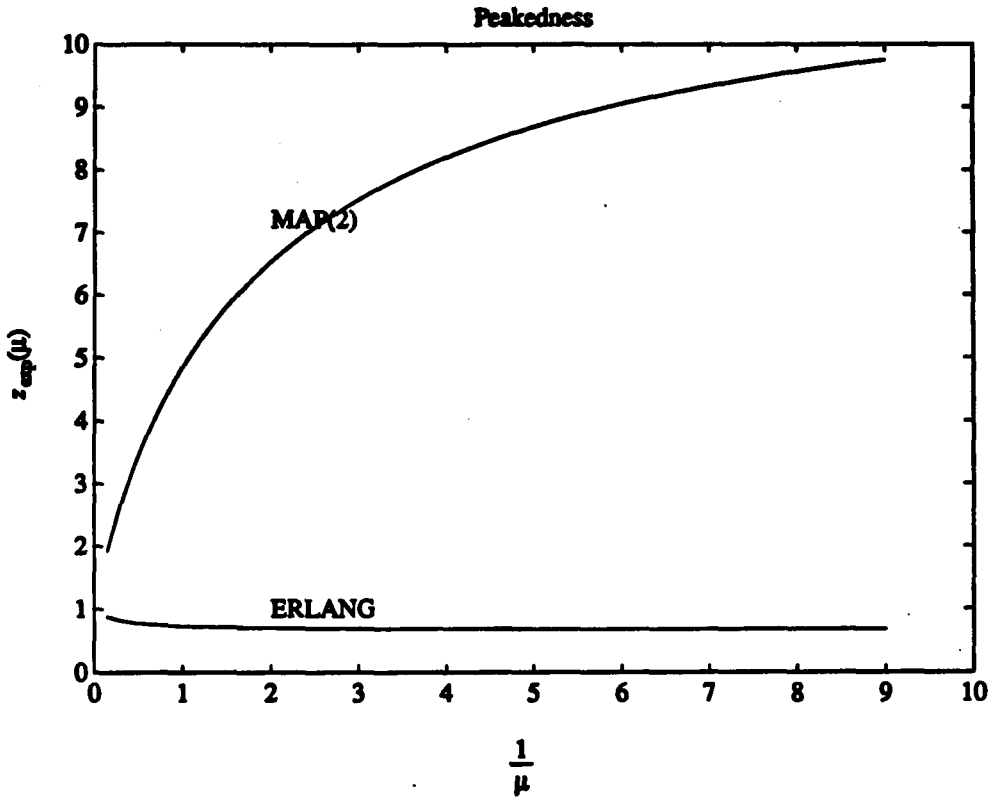

Figure 5: Exponential peakedness for Examples a. and b.

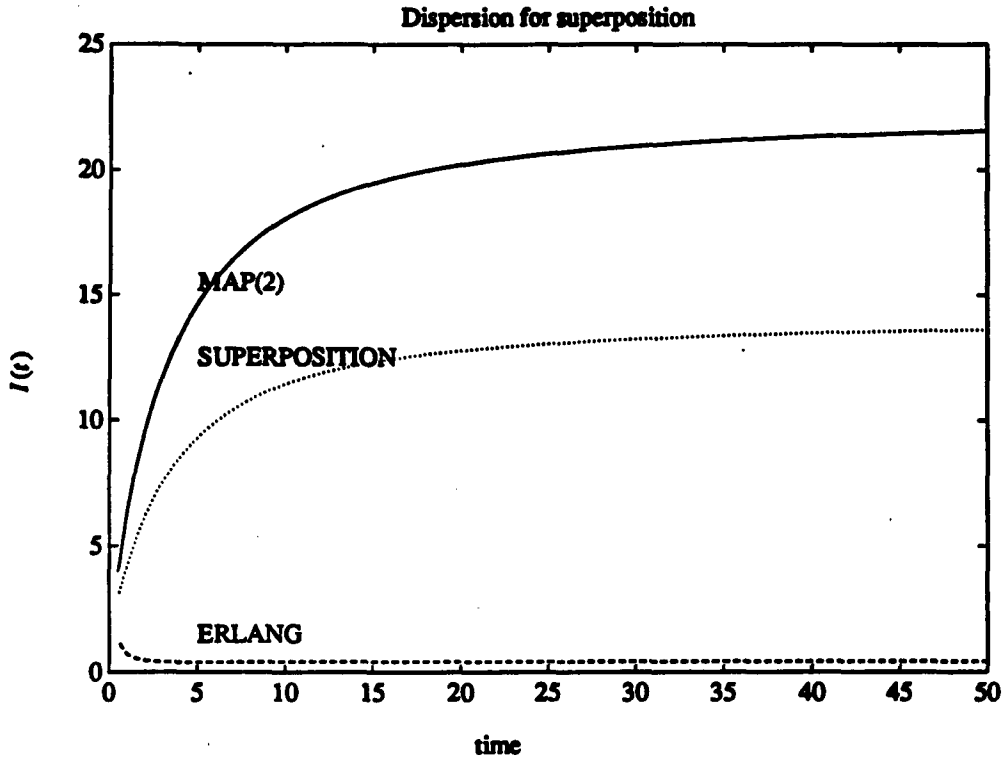

Figure 6: Dispersion function for the superposition

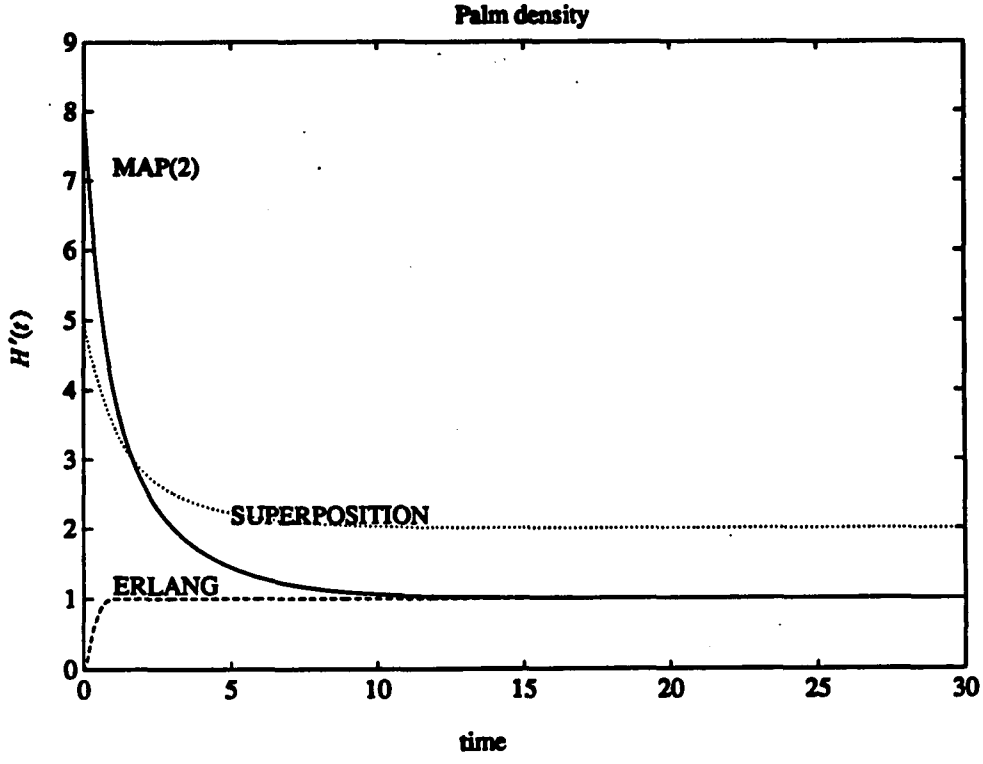

Figure 7: Palm Density for the superposition

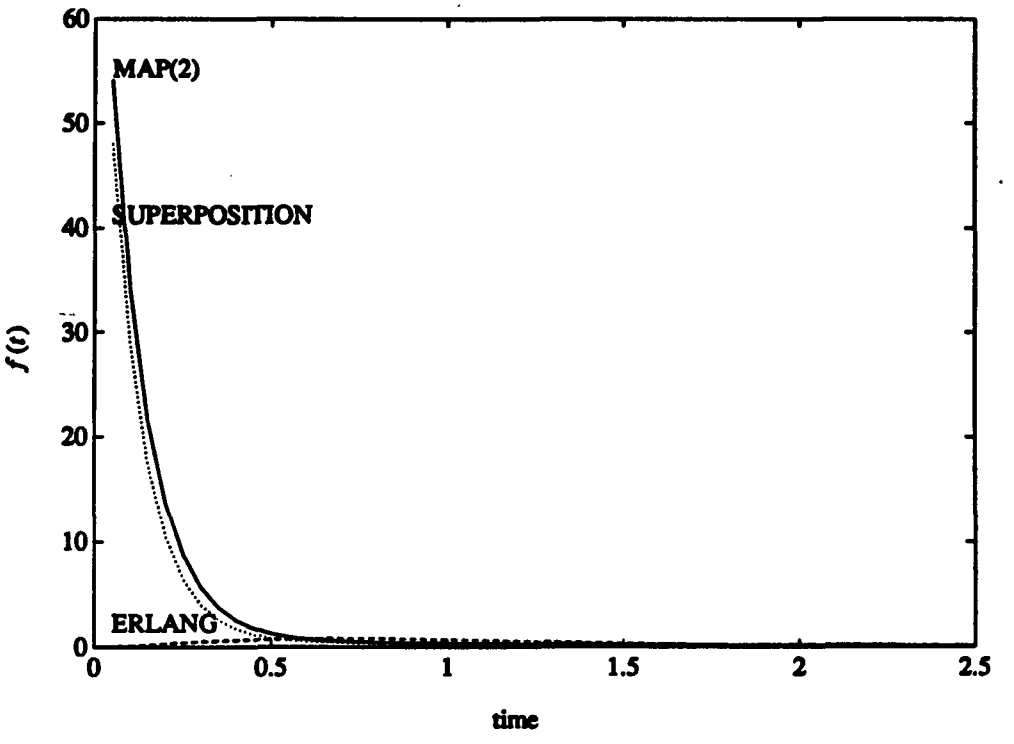

Figure 8: Density of interarrival time distribution for the superposition

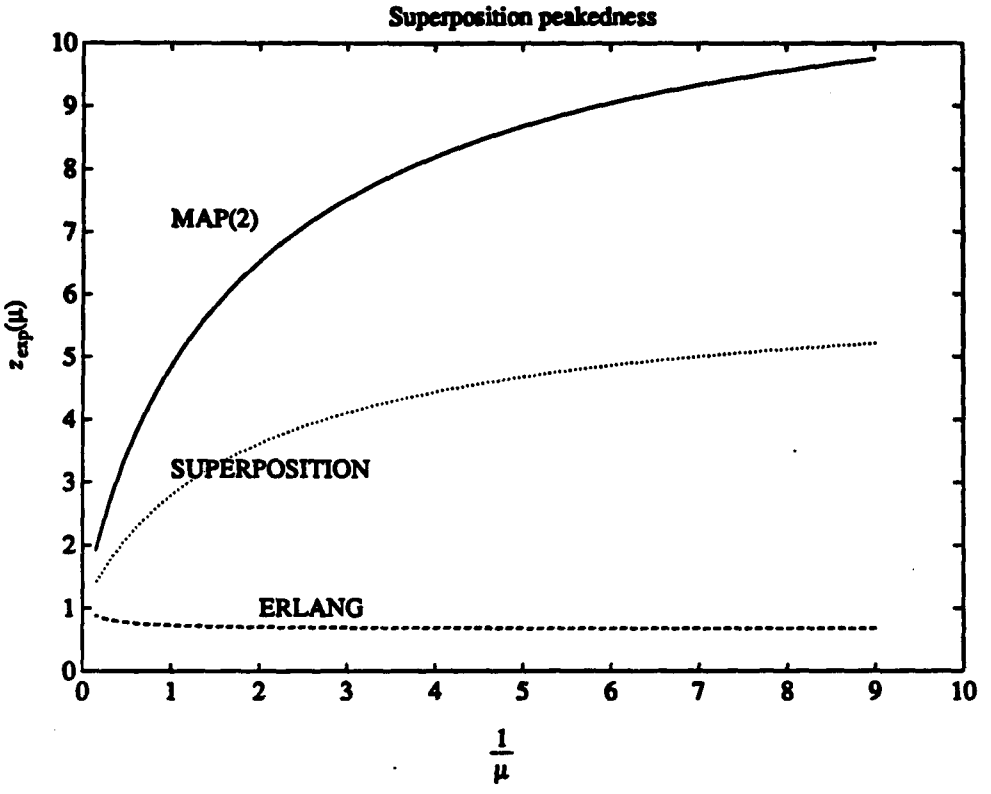

Figure 9: Exponential peakedness for the superposition

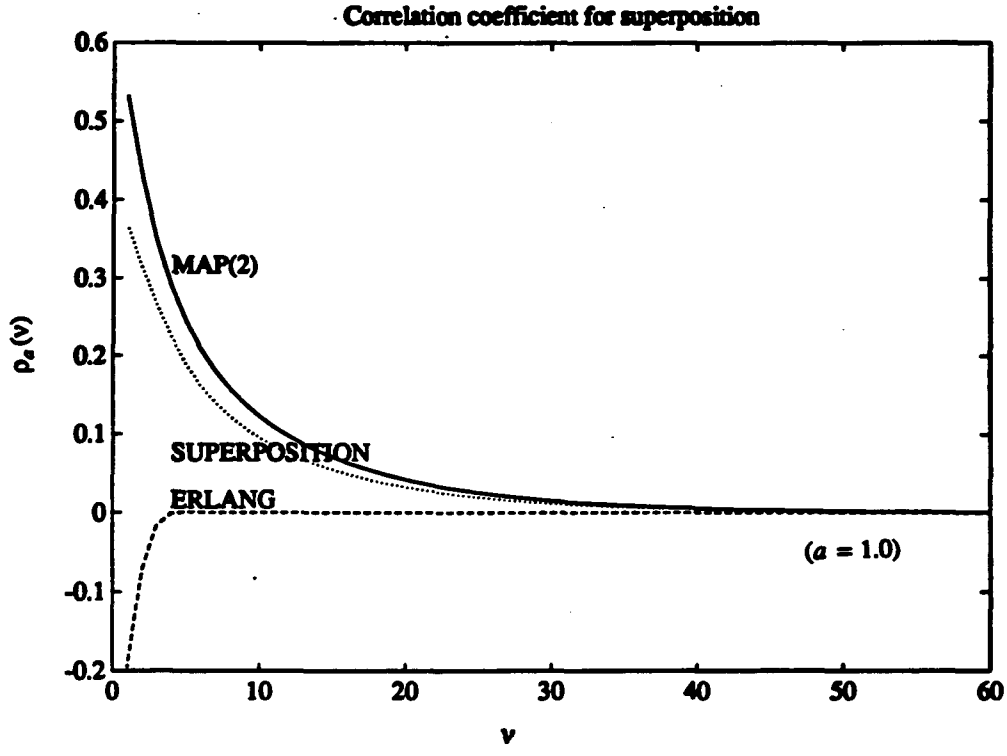

Figure 10: Correlation coefficient for the superposition.

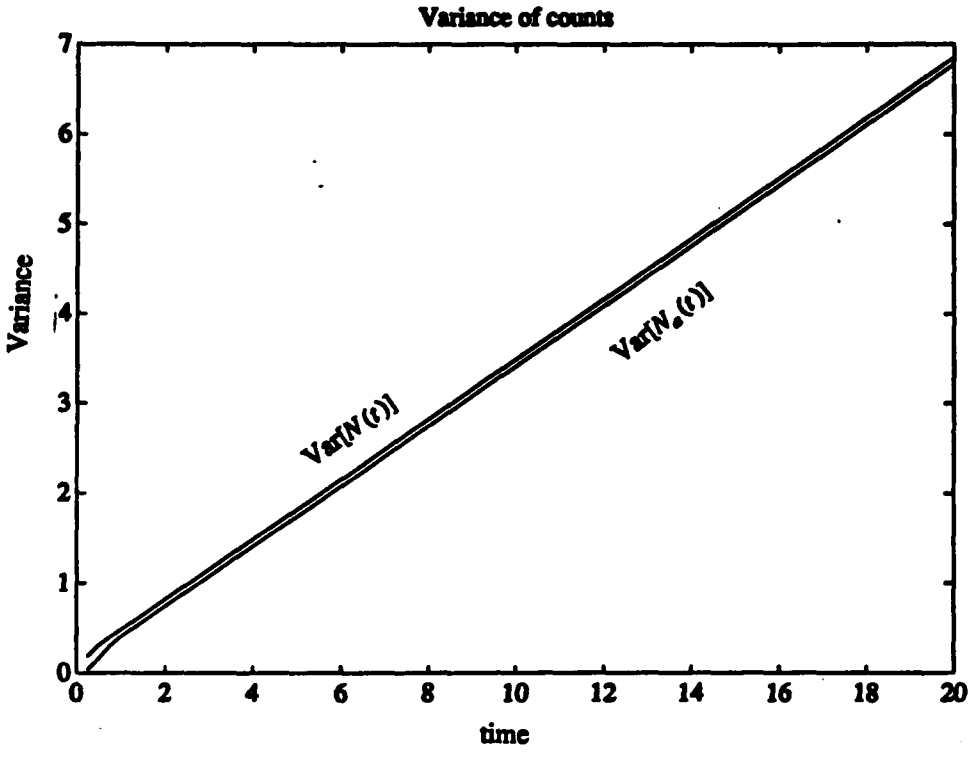

Figure 11: Variance of counts starting with an arbitrary arrival for Example a.

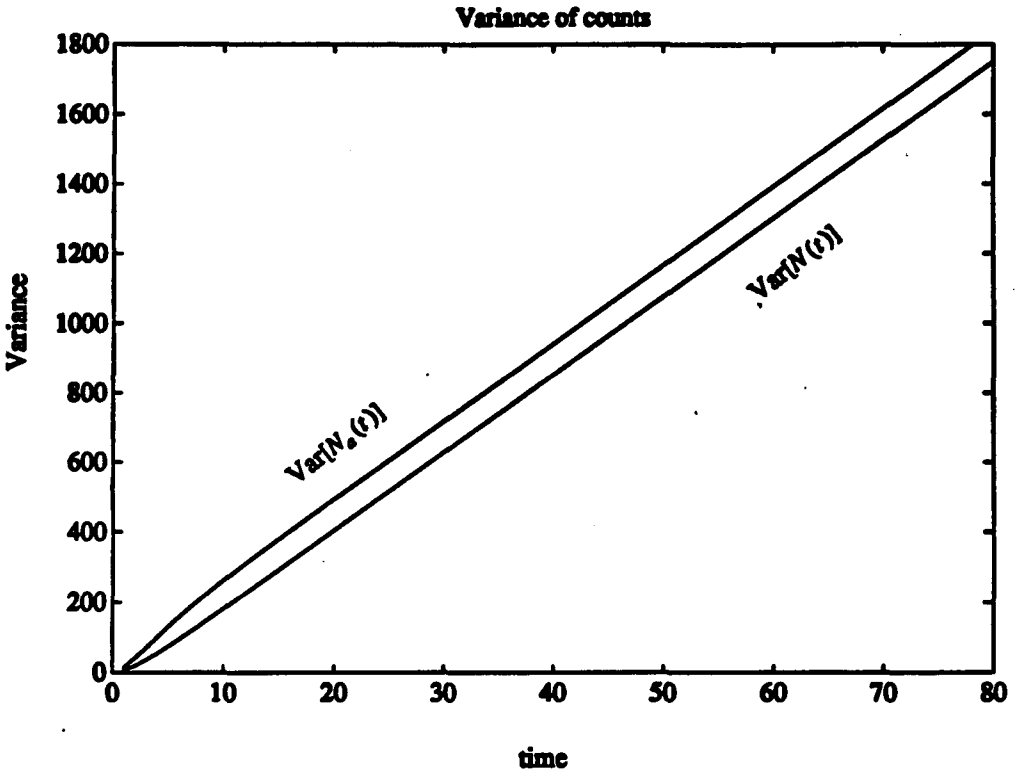

Figure 12: Variance of counts starting with an arbitrary arrival for Example b.

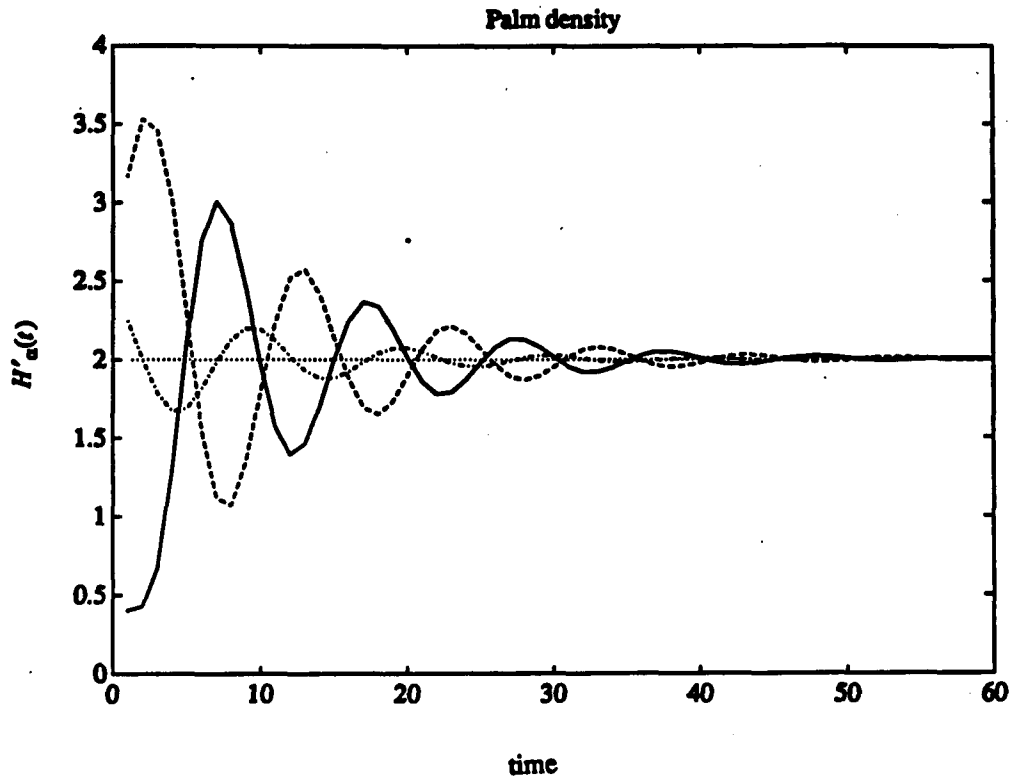

Figure 13: $H'_a(t)$ for Example (i)

(1,1)
(10,10)
(1,11)
Palm density

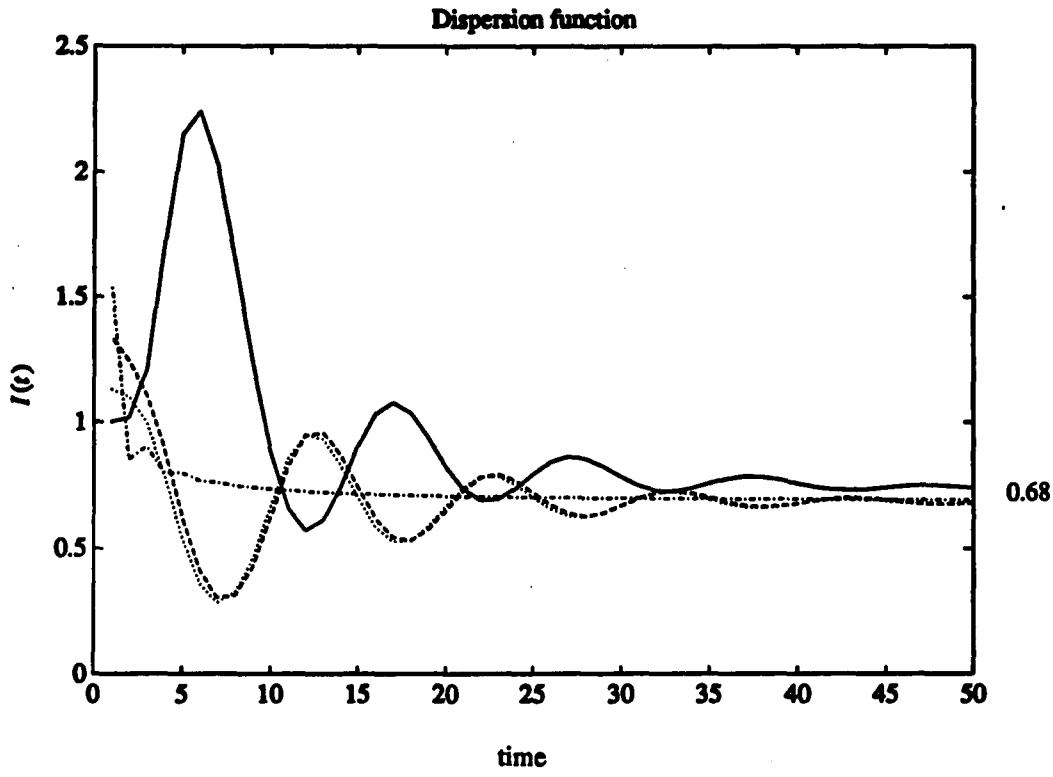

Figure 14: Dispersion function for Example (i)

(1,1)
(10,10)
(1,11)
Stationary version

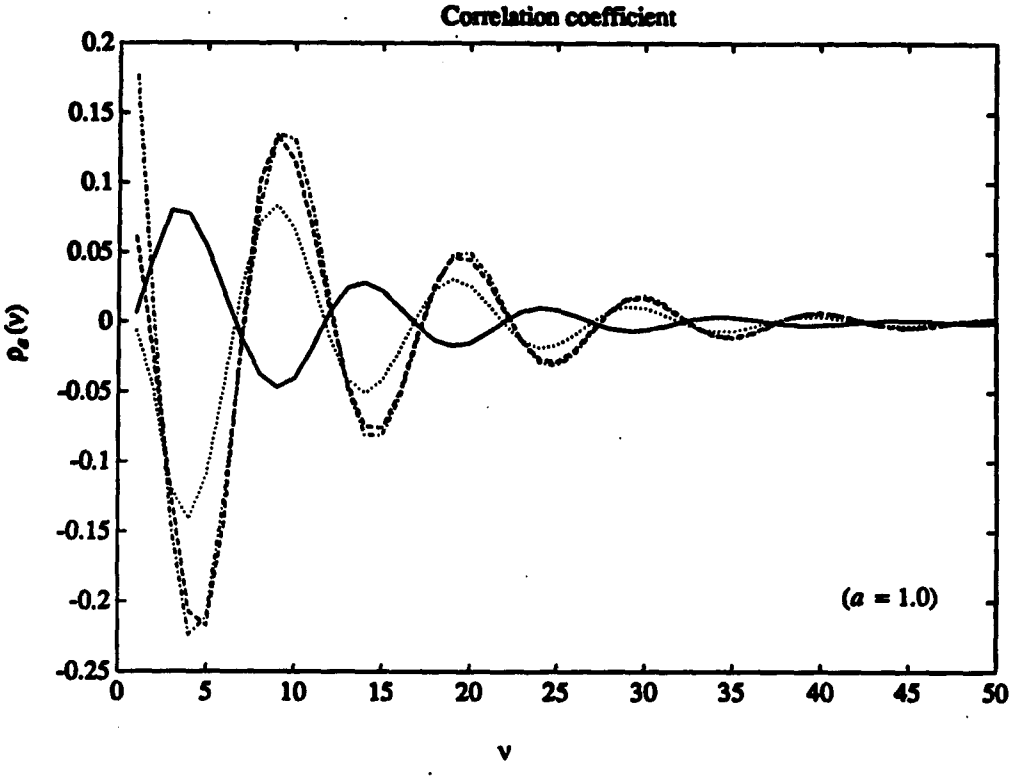

Figure 15: Correlation coefficient for Example (i)

(1,1)
(10,10)
(1,11)
Stationary version

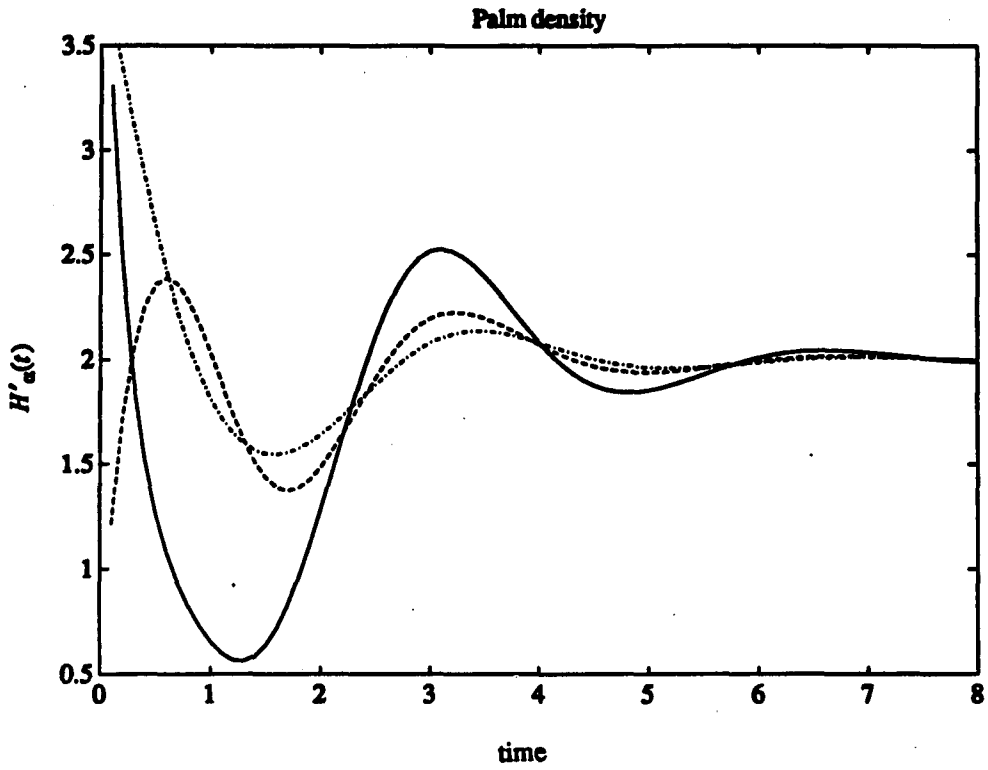

Figure 16: $H'_\alpha(t)$ for Example (ii)

(5,5)

(5,15)

Palm density

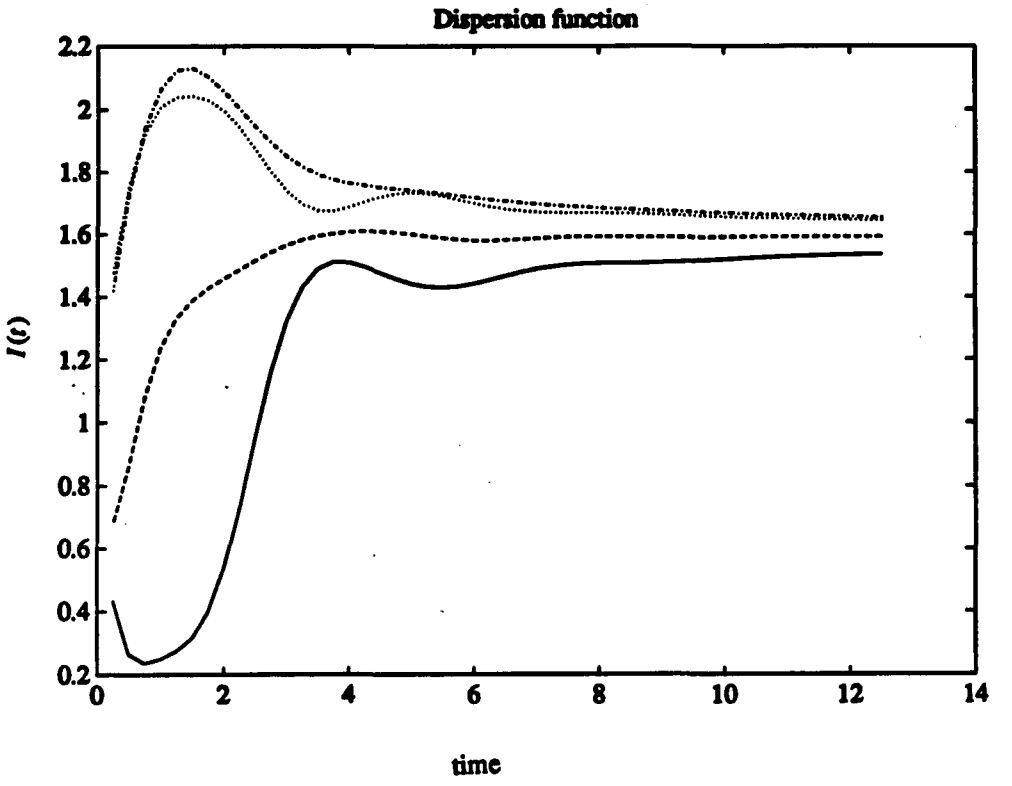

Figure 17: Dispersion function for Example (ii)

(5,5)
(5,15)
(15,15)
Stationary version

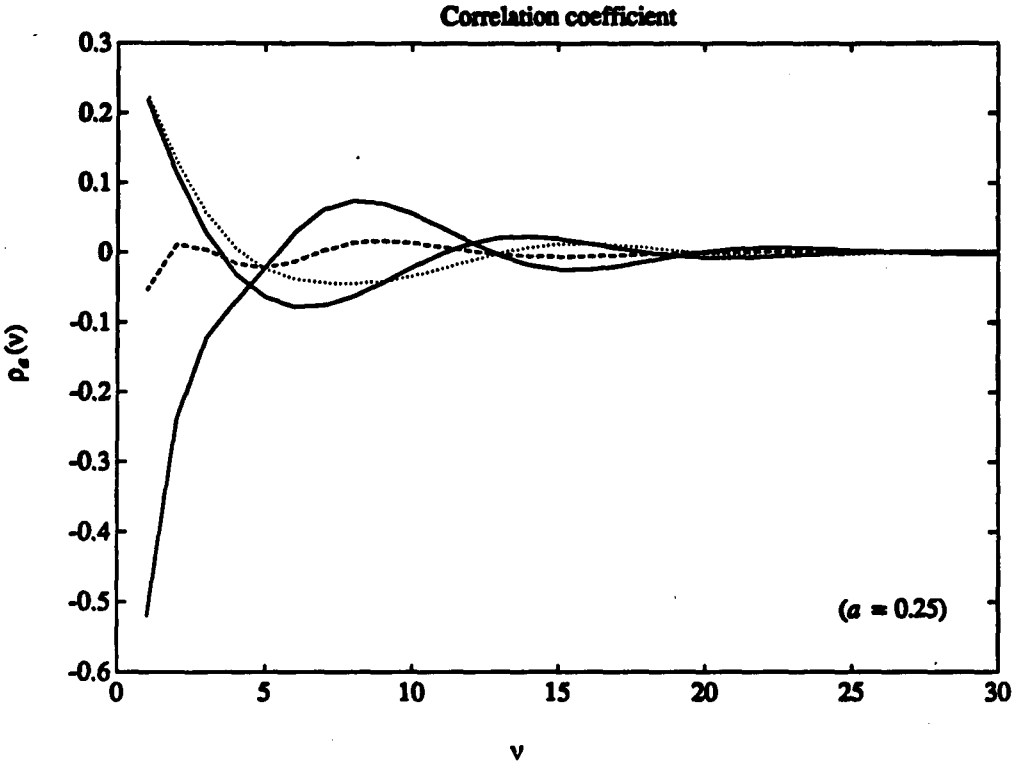

Figure 18: Correlation coefficient for Example (ii)

(5,5)
(5,15)
(15,15)
Stationary version

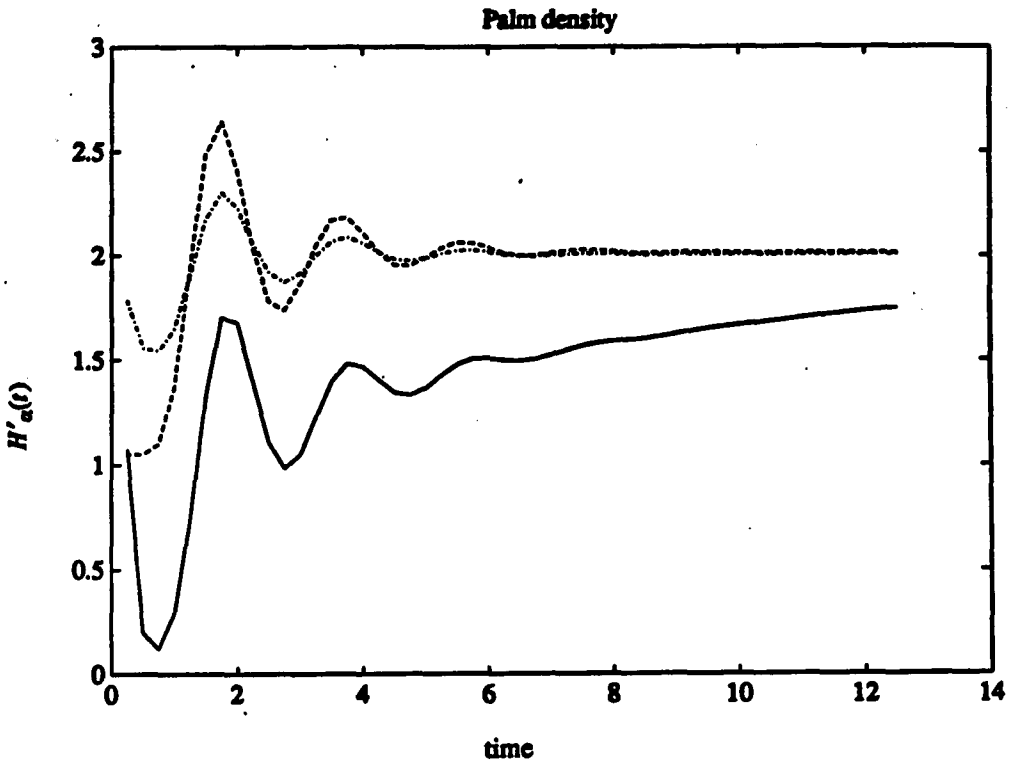

Figure 19: $H'_\alpha(t)$ for Example (iii)

(2,1)

(3,2)

Palm density

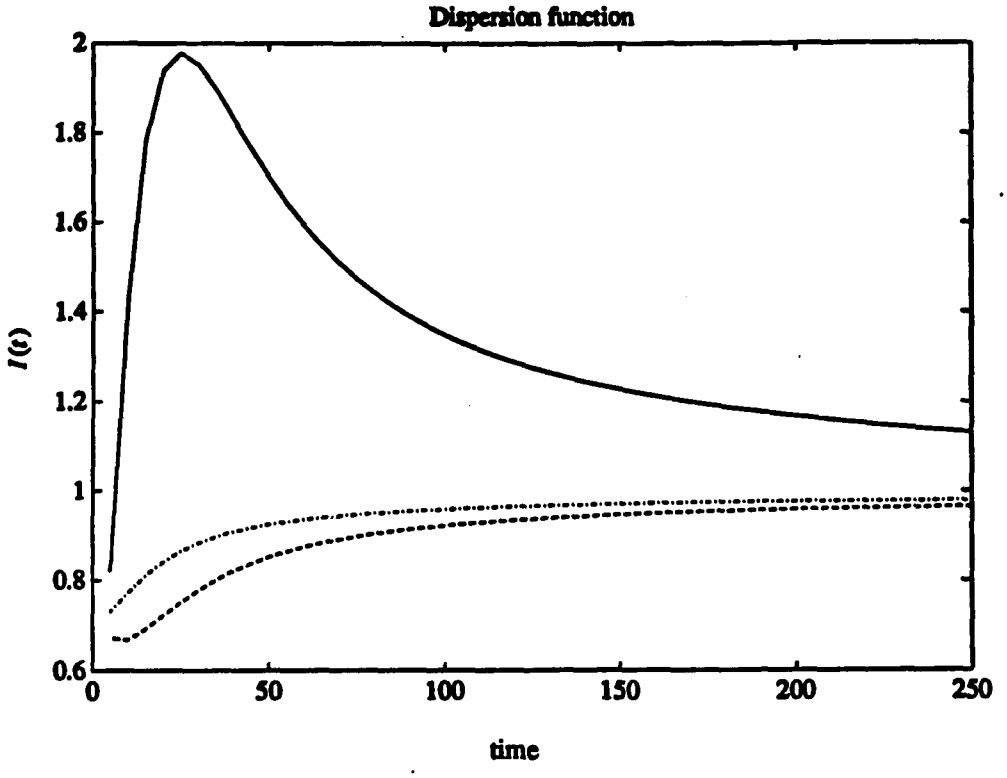

Figure 20: Dispersion function for Example (iii)

(2,1)

(3,2)

Stationary version

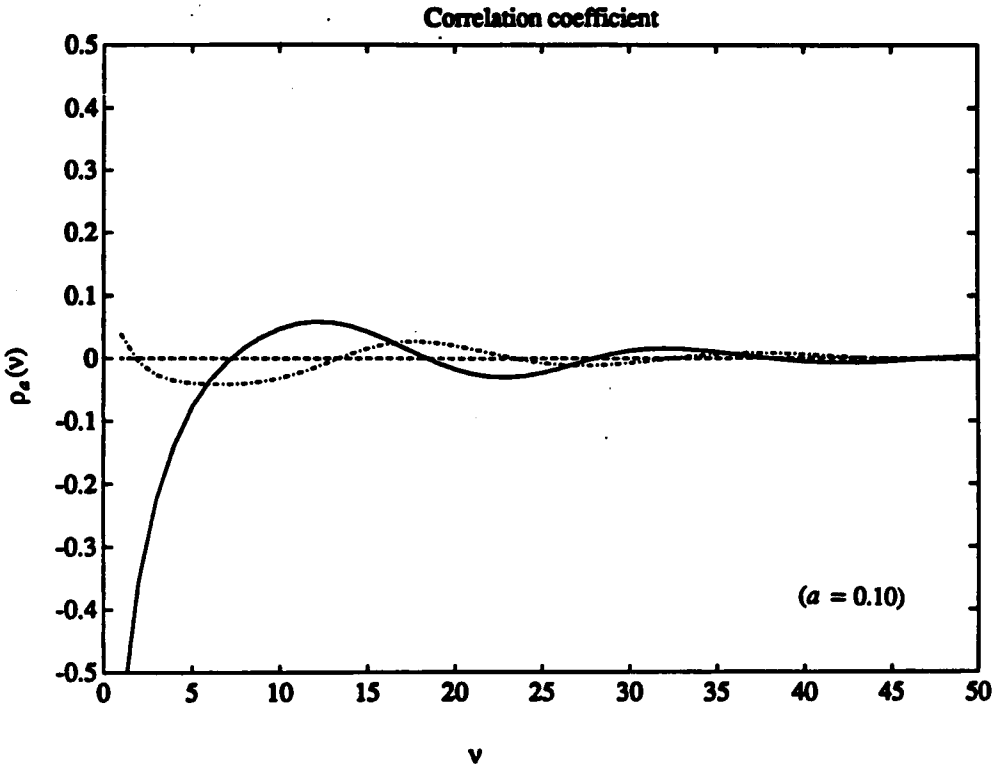

Figure 21: Correlation coefficient for Example (iii)

(2,1)

(3,2)

Stationary version

REFERENCES

[1] Eckberg, A. E., "Generalized peakedness of teletraffic processes." *Proc. Tenth. Internat. Teletraffic Conf., Montreal, Canada,* Paper No. 4.4B-3, 1983.

[2] Lucantoni, D. M., Meier-Hellstern, K. S., and Neuts, M. F., " A single server queue with server vacations and a class of non-renewal arrival processes." *Adv. Appl. Prob.,* 22, 676-705, 1990.

[3] Lucantoni, D. M., "New results on the single server queue with a batch markovian arrival process." *Stoch. Mod.,* 7, *---*, 1991.

[4] Karlin, S., A first course in Stochastic processes, 1969.

[5] Neuts, M. F., *"Structured Stochastic Matrices of M/G/1 type and Their Applications."* Marcel-Dekker Inc., New York, New York, July 1989.

[6] Neuts, M. F., *"The square wave spectrum of a Markov Renewal Process."* Forthcoming in the Proceedings of a Symposium on Stochastic Processes and their Applications in honor of Professor S. K. Srinivasan, Bombay, 1990.

[7] Neuts, M. F., Liu, D. and Narayana, S. "Local Poissonification of the Markovian Arrival Process." *Working paper,* 1990.